Kinematics of Late Cretaceous subduction initiation in the Neo-Tethys Ocean reconstructed from ophiolites of Turkey, Cyprus, and Syria

Maffione, Marco; van Hinsbergen, Douwe; de Gelder, Giovanni; van der Goes, Freek; Morris, Antony

DOI:
10.1002/2016JB013821

AGU PUBLICATIONS

JGR

Journal of Geophysical Research: Solid Earth

RESEARCH ARTICLE
10.1002/2016JB013821

Key Points:
- Late Cretaceous subduction in the western Neo-Tethys was step-shaped and composed of ~NNE-SSW and ESE-WNW subduction segments
- Subduction in the Neo-Tethys started along fracture zones within old (Triassic?) and cold lithosphere
- The eastern ~NNE-SSW trending subduction zone invaded the eastern Mediterranean to the west, leading to rotational ophiolite emplacement

Correspondence to:
M. Maffione,
m.maffione@bham.ac.uk

Citation:
Maffione, M., D. J. J. van Hinsbergen, G. I. N. O. de Gelder, F. C. van der Goes, and A. Morris (2017), Kinematics of Late Cretaceous subduction initiation in the Neo-Tethys Ocean reconstructed from ophiolites of Turkey, Cyprus, and Syria, *J. Geophys. Res. Solid Earth*, *122*, 3953–3976, doi:10.1002/2016JB013821.

Received 2 DEC 2016
Accepted 3 APR 2017
Accepted article online 5 APR 2017
Published online 9 MAY 2017

Kinematics of Late Cretaceous subduction initiation in the Neo-Tethys Ocean reconstructed from ophiolites of Turkey, Cyprus, and Syria

Marco Maffione[1,2], Douwe J. J. van Hinsbergen[1], Giovanni I. N. O. de Gelder[1,3], Freek C. van der Goes[1], and Antony Morris[4]

[1]Department of Earth Sciences, Utrecht University, Utrecht, Netherlands, [2]School of Geography, Earth and Environmental Sciences, University of Birmingham, Birmingham, UK, [3]Institut de Physique du Globe de Paris, Université Paris Diderot, Paris, France, [4]School of Geography, Earth and Environmental Sciences, Plymouth University, Plymouth, UK

Abstract Formation of new subduction zones represents one of the cornerstones of plate tectonics, yet both the kinematics and geodynamics governing this process remain enigmatic. A major subduction initiation event occurred in the Late Cretaceous, within the Neo-Tethys Ocean between Gondwana and Eurasia. Suprasubduction zone ophiolites (i.e., emerged fragments of ancient oceanic lithosphere formed at suprasubduction spreading centers) were generated during this subduction event and are today distributed in the eastern Mediterranean region along three ~E-W trending ophiolitic belts. Several models have been proposed to explain the formation of these ophiolites and the evolution of the associated intra-Neo-Tethyan subduction zone. Here we present new paleospreading directions from six Upper Cretaceous ophiolites of Turkey, Cyprus, and Syria, calculated by using new and published paleomagnetic data from sheeted dyke complexes. Our results show that ~NNE-SSW subduction zones were formed within the Neo-Tethys during the Late Cretaceous, which we propose were part of a major step-shaped subduction system composed of ~NNE-SSW and ~WNW-ESE segments. We infer that this subduction system developed within old (Triassic?) lithosphere, along fracture zones and perpendicular weakness zones, since the Neo-Tethyan spreading ridge formed during Gondwana fragmentation would have already been subducted at the Pontides subduction zone by the Late Cretaceous. Our new results provide an alternative kinematic model of Cretaceous Neo-Tethyan subduction initiation and call for future research on the mechanisms of subduction inception within old (and cold) lithosphere and the formation of metamorphic soles below suprasubduction zone ophiolites in the absence of nearby spreading ridges.

Plain Language Summary The inception of new subduction zones is one of the most critical and at the same time still unclear processes of the solid earth cycle. A major subduction initiation event started in the Late Cretaceous (~95 Ma) in the vast Neo-Tethys Ocean separating Gondwana and Eurasia landmasses. Several contrasting hypotheses have been put forward to explain the kinematics of such a regional-scale event, but most of these models invoked an unlikely simultaneous initiation of multiple subduction zones. Here we present new data from six suprasubduction zone ophiolites of Turkey, Cyprus, and Syria providing the first quantitative constraints on the kinematics of Late Cretaceous subduction initiation in the Neo-Tethys. Suprasubduction zone ophiolites are emerged fragments of oceanic crust formed during subduction inception above the embryonic subduction zone. Paleospreading directions calculated from these ophiolites indicate that the Neo-Tethyan Cretaceous subduction did not start at ~E-W trending active plate boundaries (i.e. spreading ridges) as commonly proposed, but rather along ~NNE-SSW trending fracture zones connected by ~WNW-ESE segments parallel to passive margins, in ancient (Triassic?), cold, and thick lithosphere.

1. Introduction

Subduction initiation is one of the most critical steps of the plate tectonic cycle and extensively occurred throughout the Cenozoic [e.g., *Gurnis et al.*, 2004]. However, the causes, dynamics, and kinematics of subduction initiation are still enigmatic due to the small number of clear modern examples of embryonic subduction zones, and the long, up to ~10 Myr duration of the process from incipient thrusting to self-sustaining subduction [e.g., *Gurnis et al.*, 2004; *Stern et al.*, 2012; *Arculus et al.*, 2015]. Because of this, suprasubduction zone (SSZ) ophiolites have become widely used to study subduction initiation [*Stern et al.*, 2012]. SSZ ophiolites are

dismembered fragments of oceanic lithosphere formed at suprasubduction spreading centers, which are currently exposed above sea level [e.g., *Dewey*, 1976; *Coleman*, 1981; *Casey and Dewey*, 1984; *Maffione et al.*, 2015a].

Formation of new subduction zones commonly occurs in oceanic basins along preexisting lithospheric discontinuities, i.e., transform faults or (oceanic detachment faults along) spreading ridges, which are likely the mechanically weakest sites in oceanic crust [*Toth and Gurnis*, 1998; *Hall et al.*, 2003; *Maffione et al.*, 2015b; *van Hinsbergen et al.*, 2015; *Keenan et al.*, 2016]. Investigating in ophiolites the structures that accommodated past subduction inception events is critical to constrain the force balance of subduction systems (which in turn depends on the rheology of both the lithospheric weakness zones and the upper mantle), as well as the kinematics and ultimate geological expressions of subduction initiation.

SSZ ophiolites are widespread in the eastern Mediterranean and Middle East region and form thousands of kilometers long ophiolitic belts running from Serbia to Greece and from Turkey to Oman. These ophiolites formed within the Neo-Tethys Ocean, a vast oceanic domain with intervening microcontinents separating Gondwana and Eurasia continents [e.g., *Şengör and Yilmaz*, 1981], during two major subduction initiation events in the Middle Jurassic (~170 Ma [*Schmid et al.*, 2008; *Robertson*, 2012; *Bortolotti et al.*, 2013; *Maffione et al.*, 2013, 2015b]) and Late Cretaceous (~95–90 Ma [e.g., *Searle and Cox*, 1999; *Robertson*, 2002, 2004; *Çelik et al.*, 2006; *Chan et al.*, 2007; *Karaoğlan et al.*, 2013; *van Hinsbergen et al.*, 2016 and references therein].

The main goal of this study is to reconstruct by using these SSZ ophiolites the initial geometry and subsequent kinematic evolution of the subduction system and associated SSZ spreading centers that formed in the western Neo-Tethys during the Late Cretaceous. The reconstruction of this subduction system will be critical to constraining (i) the plate boundary configuration in the Late Cretaceous, in particular the number and geometry of trenches; (ii) how these plate boundaries evolved to produce the present-day distribution of SSZ ophiolites in the eastern peri-Mediterranean region; and (iii) the nature of the preexisting weakness zones along which subduction initiated in the western Neo-Tethys. To this end, we calculate the paleospreading directions of six (plus one reported from a previous study) different suprasubduction magmatic centers that formed in the Neo-Tethys upon Late Cretaceous subduction initiation, using analysis of the orientations and paleomagnetic poles in sheeted dykes from various ophiolites of Turkey, Cyprus, and Syria.

2. Geological Setting

The ophiolites forming the focus of this study are at present incorporated in a complexly deformed orogen in the eastern Mediterranean region (Figure 1). The northern part of this orogen constitutes the Pontide mountain range of northern Turkey that contains deformed Paleozoic to Triassic basement interpreted to derive from the Sakarya continental block that collided with Eurasia in Triassic to Early Jurassic time [*Şengör and Yilmaz*, 1981; *Sayıt and Göncüoglu*, 2013; *Okay et al.*, 2014; *Dokuz et al.*, 2017]. These units are overlain by a Mesozoic sedimentary cover, including Jurassic to Cenozoic arc volcanic rocks [e.g., *Okay et al.*, 2013; *Dokuz et al.*, 2017]. To the north, the Pontides are separated from Eurasia by the Cretaceous-to-Paleogene Black Sea back-arc basin [*Okay et al.*, 1994; *Munteanu et al.*, 2011; *Nikishin et al.*, 2015; *Sosson et al.*, 2016], while to the South they are fringed by a belt known as the İzmir-Ankara suture zone. This suture zone contains a chaotic mélange of serpentinites, deep marine sediments, and ophiolite fragments, which demarcates the location where the northern branch of the eastern Mediterranean Neo-Tethys subducted northward since Middle Jurassic time [*Şengör and Yilmaz*, 1981]. Within the İzmir-Ankara suture zone, a series of ophiolites with Middle Jurassic crustal ages and metamorphic soles has been recognized, whose plate kinematic setting remains debated but that show ages comparable to the ophiolites of the Balkans and Greece [*Çelik et al.*, 2011; *Topuz et al.*, 2013, *Çörtük et al.*, 2016].

The ophiolites analyzed in this study are distributed south of the İzmir-Ankara suture zone and form the highest structural unit of a dominantly continental crust-derived orogen known as the Anatolide-Tauride belt [e.g., *Şengör and Yilmaz*, 1981; *Okay*, 1986; *Okay and Whitney*, 2010; *Plunder et al.*, 2013, 2016, *van Hinsbergen et al.*, 2016]. These ophiolites have a SSZ geochemical signature and crustal ages that are consistently clustered around 95–90 Ma (see reviews in, e.g., *Robertson* [2002], *Moix et al.* [2008], and *van Hinsbergen et al.* [2016]). These ophiolites are underlain by thin and disrupted metamorphic soles with Ar/Ar cooling ages that are comparable to those of the ophiolitic crust [*van Hinsbergen et al.*, 2015, 2016].

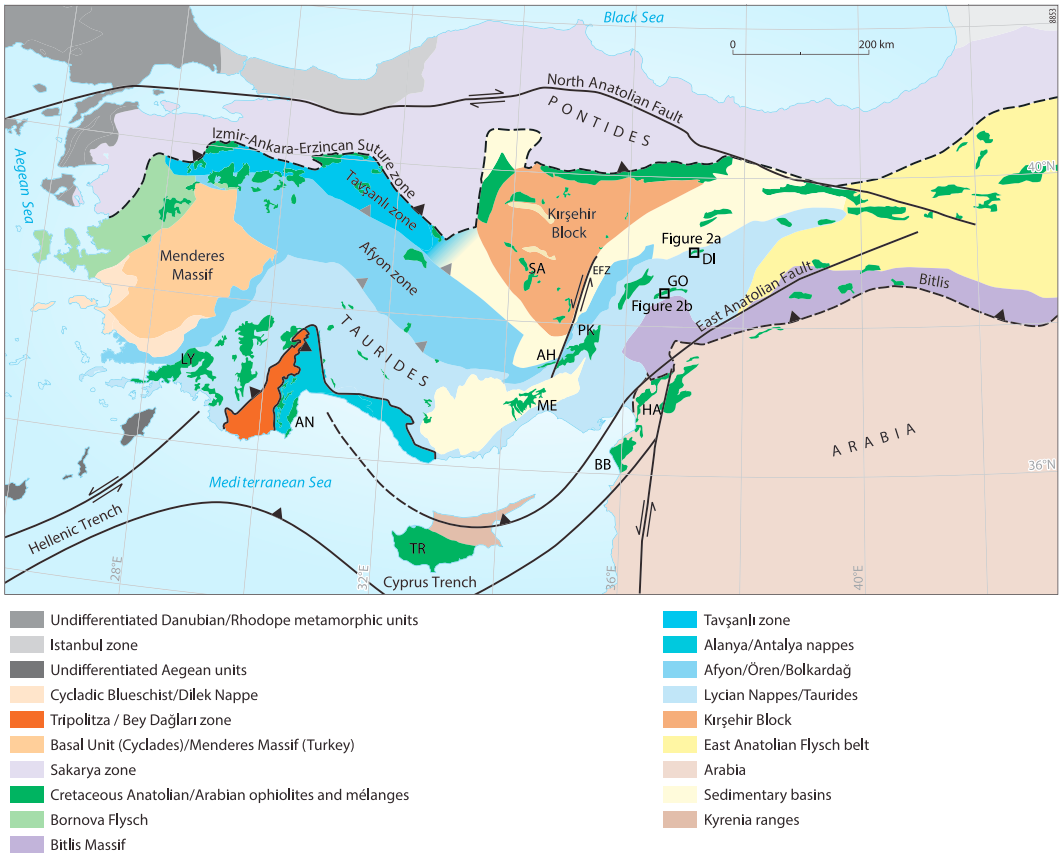

Figure 1. Main tectono-stratigraphic domains and tectonic structures of Turkey and surrounding regions, showing the distribution of the Late Cretaceous Neo-Tethyan ophiolites. DI, Divriği ophiolite; GO, Göksun ophiolite; AH, Alihoca ophiolite; SA, Sarıkaraman ophiolite; LY, Lycian ophiolite; AN, Antalya ophiolite; ME, Mersin; PK, Pozantı-Karsantı ophiolite; HA, Hatay ophiolite; BB, Baer-Bassit ophiolite; TR, Troodos ophiolite; EFZ, Ecemiş fault zone.

Ophiolitic mélanges of the İzmir-Ankara suture zone that structurally overlie, as well as the mélanges that structurally underlie the Cretaceous ophiolites, contain radiolarian cherts as old as the Early Triassic [*Tekin et al.*, 2002, 2016; *Tekin and Göncüoğlu*, 2007]. This indicates that the eastern Mediterranean Neo-Tethys Ocean had been forming since at least Early Triassic time (~245 Ma), probably when the Sakarya block of the Pontides separated from Gondwana and drifted toward Eurasia [e.g., *Dokuz et al.*, 2017].

The Anatolide-Tauride belt consists of metamorphosed and nonmetamorphosed continent-derived units that from structurally high to low positions include the Kırşehir block and Tavşanlı zone, both showing ~85 Ma metamorphic ages, the Afyon zone with ~65 Ma metamorphic ages, and the Tauride fold-thrust belt (including the Menderes Massif) that underthrust and accreted to the Eurasian margin in Paleogene time (see review in *van Hinsbergen et al.* [2016]) (Figure 1). The Kırşehir Block and Tavşanlı zone in the north may have been separated from the Afyon zone, which formed the promontory of the Tauride continental platform, by another, few hundred kilometer-wide oceanic basin conceptually known as the Intra-Tauride ocean. The Upper Cretaceous ophiolites overlying the Taurides are frequently inferred to derive from this Intra-Tauride ocean basin [e.g., *Robertson et al.*, 2009; *Parlak et al.*, 2013; *Barrier and Vrielynck*, 2008; *Menant et al.*, 2016]. However, a recent plate kinematic reconstruction [*van Hinsbergen et al.*, 2016] suggested that derivation of ophiolites from an Intra-Tauride basin is plate kinematically unlikely and not required to explain the orogenic structure. According to *van Hinsbergen et al.* [2016], these ophiolites, including those lying on the Lycian nappes (Lycian ophiolites), on the northern Taurides (Alihoca and Divriği ophiolites), as well as on the metamorphosed Afyon, Tavşanlı, and Kırşehir units (e.g., the Sarıkaraman ophiolite), may be part of a single oceanic thrust sheet that rooted in the Izmir-Ankara suture and was emplaced from the Late Cretaceous until the Eocene onto Gondwana-derived terranes. The modern, wide areal dispersion of these ophiolites may (at least

in part) be explained by regional Late Cretaceous to Miocene extension [e.g., *Bozkurt and Oberhänsli*, 2001; *van Hinsbergen et al.*, 2010, 2016; *Gautier et al.*, 2008; *Lefebvre et al.*, 2011, 2015].

Along the southwestern coast of Turkey, around the Bay of Antalya, ophiolites and an underlying fold-and-thrust belt are found, known as the Antalya-Alanya nappes (Figure 1). Structural and stratigraphic evidence demonstrates that these ophiolites and the underlying fold-and-thrust belt were emplaced northward over the Tauride platform until latest Cretaceous times, with their frontal thrust being sealed by Eocene sediments [e.g., *Okay and Ozgul*, 1984]. The Antalya ophiolite and its dismembered metamorphic sole have the same ~95–90 Ma ages as the rest of the Anatolian ophiolites [e.g., *Çelik et al.*, 2006], but their emplacement direction clearly shows that they were derived from a separate subduction segment. The Alanya nappes comprise a continent-derived HP-LT metamorphic complex [*Okay and Ozgul*, 1984] with ages of ~85–82 Ma, interpreted as a far-traveled, deeply underthrust relict of Tauride platform rocks [*Cetinkaplan et al.*, 2016].

Other Upper Cretaceous ophiolites of the southeastern Taurides—including the Göksun ophiolite—are located to the north of the Bitlis massif and are overlying meta-sedimentary rocks known as the Malatya-Keban units (Figure 1). Both the ophiolites and the overlying metamorphics are intruded by Campanian (~85–81 Ma) granitoids [*Parlak et al.*, 2004; *Parlak*, 2006; *Karaoğlan et al.*, 2016], indicating that this region was already involved in orogenesis in Late Cretaceous time, well before the Paleogene arrival of the northern ophiolites on the Taurides.

In the southeastern Taurides along the northern front of undeformed Arabia lies the Bitlis massif (Figure 1). This, as well as the Arabian continent itself are also overlain by Cretaceous ophiolites, once again with ~95–90 Ma crustal and sole ages [e.g., *Parlak et al.*, 2009]. The Bitlis massif, in addition, underwent Late Cretaceous HP-LT, eclogite, and blueschist-facies metamorphism, the former dated at 85–82 Ma and cooling after blueschist metamorphism continuing until ~70 Ma [*Oberhänsli et al.*, 2012, 2014]. The age of HP-LT metamorphism in the Bitlis massif is thus similar to that in the Alanya nappes and to the granitoid ages of the southeastern Taurides intruding the Malatya-Keban metamorphics and is likely related to the same orogenic event [*Karaoğlan et al.*, 2016; *Cetinkaplan et al.*, 2016].

Ophiolites to the south of the Bitlis massif, including the Hatay and Baer-Bassit ophiolites of Turkey and Syria, respectively, overlie the undeformed Arabian foreland (Figure 1). The emplacement age of these ophiolites is constrained by Maastrichtian sediments sealing the obduction thrust [*Al Riyami and Robertson*, 2002; *Kaymakcı et al.*, 2010]. It is widely perceived that the Troodos ophiolite of Cyprus (Figure 1) forms the westward continuation of the Hatay and Baer-Bassit ophiolites. The Troodos ophiolite has crustal ages of 92–90 Ma [*Mukasa and Ludden*, 1987], similar to the ages retrieved from metamorphic sole relics in the juxtaposed Mamonia Complex [*Chan et al.*, 2007]. The Mamonia Complex is an accretionary prism including ocean and continental passive margin-derived rocks with ages ranging from Triassic to Early Cretaceous [e.g., *Bailey et al.*, 2000]. The juxtaposition of the Troodos ophiolite with the Mamonia Complex has been constrained at the latest Cretaceous based on uppermost Maastrichtian mass flow deposits sealing the contact between the two units [*Swarbrick and Naylor*, 1980]. The origin and provenance of the Mamonia Complex mélange are, however, still debated. In the Miocene fold-and-thrust belt in northern Cyprus, known as the Kyrenia Range, continental passive margin sediments are found that underwent low-grade metamorphism in the Late Cretaceous, prior to extensional exhumation to the seafloor in latest Cretaceous time [e.g., *Robertson et al.*, 2012]. Because of similarities in the ophiolite structure as well as a Late Cretaceous major counterclockwise rotation phase demonstrated paleomagnetically [e.g., *Clube and Robertson*, 1986], the Troodos ophiolite is widely considered to have been part of a microplate together with the Baer-Bassit and Hatay ophiolites [e.g., *Morris et al.*, 2002, 2006; *Inwood et al.*, 2009a]. Contrary to the Hatay and Baer-Bassit ophiolites, however, Cyprus is at present not part of the African-Arabian plate but is located in the fore arc of the eastern Mediterranean subduction zone (Figure 1).

3. Sampling and Methods

In this study, we present new paleomagnetic data from the sheeted dyke complexes of three different ophiolites in central Turkey: the Divriği, Alihoca, and Göksun ophiolites (Figure 1 and Table 1). All sampled dykes have a doleritic composition and magmatic texture. At all sampled sites, one core per dyke was drilled, and the orientations of at least 10 dykes were measured to calculate a site mean dyke direction. Based on these new data, we determined the tectonic rotation parameters and the initial (predeformation) dyke

Table 1. New Paleomagnetic Results From the Divriği, Alihoca, and Göksun Ophiolites and Recalculated Directions for the Baer-Bassit Ophiolite[a]

Site	Latitude	Longitude	Strike/Dip	δS	N	N_{45}	D	dD	I	dI	k	α_{95}	K	A_{95}	A_{95min}	A_{95max}
Divriği ophiolite																
DIV01	39.378528°	37.854573°	295/52	6.4	30	26	330.6	5.1	36.9	7	38.1	4.7	35.7	4.8	3.3	10.5
DIV02	39.378528°	37.854573°	266/66	7.1	40	39	331.5	3.9	36.9	5.3	41.3	3.6	41.3	3.6	2.8	8.2
DIV03	39.378528°	37.854573°	262/67	4.7	14	14	343.2	4.0	35.3	4.0	205.8	2.8	220.1	2.7	4.2	15.6
DIV06	39.378528°	37.854573°	281/71	6.8	31	30	349.7	5.7	24.4	9.7	20.6	5.9	23.4	5.6	3.1	9.6
Average DIV01/02/03/06	39.378528°	37.854573°	265/64	5.5	115	95	338.0	3.1	33.3	4.5	23.9	3.0	26.0	2.9	1.9	4.7
DIV04	39.366639°	37.859722°	235/84	8.2	6	6	297.7	38.5	79.4	6.9	90.2	7.1	29.4	12.6	5.9	26.5
DIV05	39.369167°	37.860750°	256/70	5.6	6	6	320.4	7.5	46.9	8.0	111.9	6.4	103.1	6.6	5.9	26.5
DIV07	39.244111°	37.777417°	255/60	6.2	24	23	321.0	4.7	6.5	9.2	30.3	5.6	43.2	4.7	3.4	11.4
Alihoca ophiolite																
AH	37.511596°	34.821244°	013/89	13.7	26	25	349.5	7.6	57.5	5.5	35.6	4.9	24.8	5.9	3.3	10.8
Göksun ophiolite																
GOK01[b]	38.120732°	36.864106°	237/85	4.0	31	24	000.5	7.4	47.5	7.7	22.1	6.4	21.6	6.5	3.4	11.1
GOK02, GOK03	38.134838°	36.874114°	237/85	4.0	147	145	039.0	1.9	23.0	3.3	34.5	2.0	39.5	1.9	1.6	3.6
Baer-Bassit ophiolite[a]																
North Coast (A)			123/86	7.4	23	23	068.8	5.1	−33.7	7.5	28.2	5.8	39.4	4.9	3.4	11.4
North Coast (B)			118/89	5.0	11	11	108.2	5.1	−34.6	7.3	63.1	5.8	89.8	4.8	4.6	18.1
Bassit Road			329/81	13.3	50	50	024.3	5.0	−88.5	1.8	114.1	1.9	31.0	3.7	2.5	7.0
Quastal Maaf			325/20	5.0	16	16	200.5	3.4	−19.5	6.2	59.2	4.8	120.7	3.4	4.0	14.3

[a]Data recalculated from *Morris et al.* [2002] using a parametric sampling of original data. δS is the 95% confidence around the mean pole to dyke calculated from field measurements of at least 10 adjacent dykes at each site. N, total number of processed specimens; N_{45}, number of specimens used for the calculation of the mean values after filtering with a 45° cutoff [*Johnson et al.*, 2008]. D, d_{Dx}, mean declination and associated error; I, d_{Ix}, mean inclination and associated error; k and α_{95}, precision parameter and semiangle of the 95% cone of confidence around the computed site mean direction; K and A_{95}, precision parameter and semiangle of the 95% cone of confidence around the mean virtual geomagnetic pole; A_{95max} and A_{95min}, maximum and minimum value of A_{95} expected from paleosecular variation of the geomagnetic field calculated after *Deenen et al.* [2011].
[b]Discarded site due to possible present-day remagnetization.

orientations from which we infer the paleospreading directions. Furthermore, paleospreading directions were also determined for the Troodos (Cyprus), Hatay (Turkey), and Baer-Bassit (Syria) ophiolites based on a reinterpretation of published paleomagnetic data.

3.1. Studied Ophiolites

3.1.1. Divriği Ophiolite

The Divriği ophiolite rests on the northern part of the Lower Carboniferous-Campanian Tauride carbonate platform rocks of east-central Anatolia (Figure 1). The ophiolite is composed of mantle ultramafics and gabbroic cumulates, isotropic gabbro, and sheeted dykes overlain by a Campanian-Maastrichtian volcano-sedimentary sequence [*Yilmaz and Yilmaz*, 2004; *Parlak et al.*, 2006]. U-Pb zircon ages of 88.8 ± 2.5 Ma from the cumulate gabbros are comparable with ^{40}Ar-^{39}Ar ages of the underlying metamorphic sole (87–89 Ma [*Parlak et al.*, 2013]) and support formation of the ophiolite during subduction initiation in a fore-arc setting [*Parlak et al.*, 2013]. The ophiolite and metamorphic sole overlie the Yeşiltaşyayala mélange, which includes fragments of metamorphic sole rocks incorporated into a serpentinized matrix [*Uçurum*, 2000]. A number of discrete, nonmetamorphic, alkaline dykes with ^{40}Ar-^{39}Ar ages of ~76 Ma [*Parlak et al.*, 2013] crosscut both the ophiolite and the underlying metamorphic sole and are interpreted to have derived from fertile mantle melts produced before ophiolite emplacement [*Parlak et al.*, 2006]. Finally, A-type granitoids with U-Pb zircon ages of ~69 Ma [*Parlak et al.*, 2013] intrude both the ophiolite and underlying ophiolitic mélange and are unconformably overlain by Eocene basal conglomerates [*Yilmaz et al.*, 2001]. Field and age relationships indicate an emplacement age of the Divriği ophiolite onto the northern Taurides of ~65 Ma and younger [*Parlak et al.*, 2013; *Robertson et al.*, 2013].

A total of 151 paleomagnetic core samples were collected at seven sites (DIV01 to DIV07) distributed throughout the sheeted dyke complex of the Divriği ophiolite, near the village of Günes (Table 1 and Figure 2a). Sampled dykes are between 30 and 150 cm thick, frequently show chilled margins on one side of the dyke, and are steeply dipping approximately to the North.

3.1.2. Alihoca Ophiolite

The Alihoca ophiolite is presently located above the northern side of the Tauride thrust belt, in the foothills of the Bolkar Mountains (Figure 1). The Alihoca ophiolite displays an ~1500 m thick dismembered ophiolite

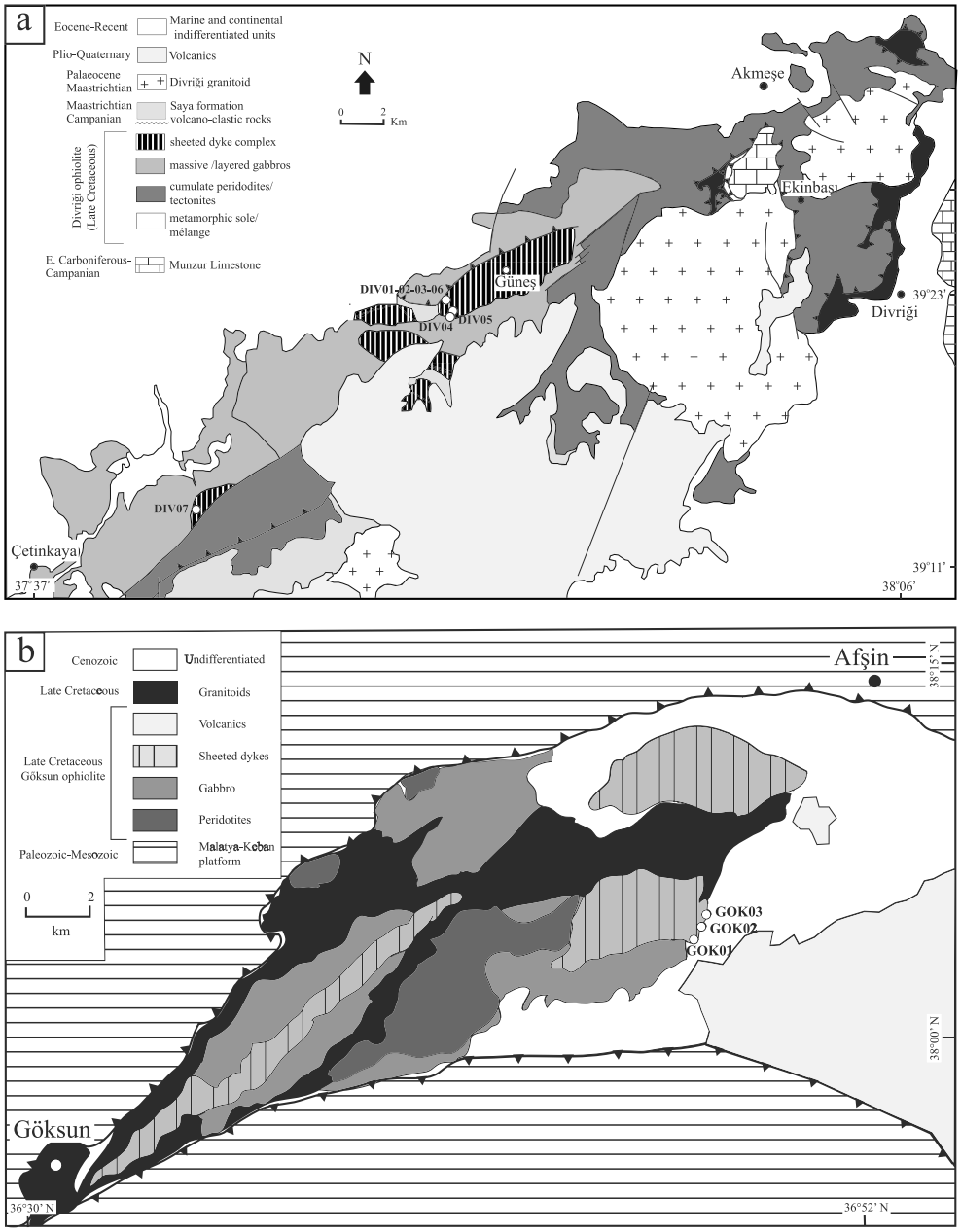

Figure 2. Geological maps of (a) the Divriği ophiolite, modified from *Parlak et al.* [2006], and (b) the Göksun ophiolite, modified after *Parlak et al.* [2004], showing the main lithologies and sampling sites.

pseudostratigraphy, composed of deformed mantle peridotites (harzburgites with minor dunites), layered-to-isotropic gabbros, sheeted dykes, and a very thin (and locally absent) volcanic sequence. Available ages from pegmatitic gabbros (92.38 ± 0.48 Ma from U-Pb on zircon [*Gürer et al.*, 2016]), and late stage mafic dykes cutting (in adjacent localities) the metamorphic sole (90.8 ± 0.8 Ma from hornblende $^{40}Ar/^{39}Ar$ [*Dilek et al.*, 1999]), are comparable to ophiolitic crustal ages across Turkey.

The Alihoca ophiolite rests tectonically on an ophiolitic mélange that consists of dolerites, basalts, radiolarian cherts, and Triassic to Cretaceous limestones within a serpentinite matrix. The mélange is cut by the Eocene Horoz granitoid [*Kadioglu and Dilek*, 2010]. The emplacement of the Alihoca ophiolite onto the Anatolide-Taurides platform may have occurred as early as the Campanian [*Gürer et al.*, 2016].

A total of 28 paleomagnetic samples were collected at one site (AH) within the sheeted dyke complex exposed along the road to Ardicli village (Table 1). Here the sheeted dyke sequence is no thicker than few hundreds of meters and contains subvertical dykes striking NNE-SSW to N-S, with individual dykes being 30 to 100 cm thick on average.

3.1.3. Göksun Ophiolite

The Göksun ophiolite is located in the southeastern Taurides and is exposed in a tectonic window below the metamorphic Paleozoic-Mesozoic Malatya-Keban platform (Figure 1). The Göksun ophiolite exposes a well-preserved and thick sequence composed of a condensed mantle sequence overlain by isotropic-to-layered gabbro, a sheeted dyke complex, and a thin volcanic sequence [*Parlak*, 2006]. Pelagic microfossils found interlayered with the volcanic sequence indicate a minimum Campanian age of the ophiolitic crust [*Perinçek and Kozlu*, 1984]. Both the ophiolite and Malatya-Keban platform rocks are intruded by ~88–85 Ma [*Parlak*, 2006] I-type calc-alkaline granitoids. The current structural relationship with the ophiolite located below the Malatya metamorphics has led to models whereby the ophiolite accreted below the Malatya metamorphics [e.g., *Parlak*, 2006]. This does not explain the metamorphism of the Malatya units; furthermore, accretion of an ophiolite, which represents a thinned but otherwise full oceanic lithosphere, to an overriding plate is geodynamically implausible. There is no detailed structural reconstruction of the eastern Tauride fold-thrust belt, but we assume that the current situation is the result of out-of-sequence thrusting and that the Göksun ophiolite was obducted onto the Taurides platform in the Late Cretaceous in the short time span between oceanic crust formation and intrusion of the granitoids.

A total of 178 paleomagnetic samples were collected at three adjacent sites (GOK01, GOK02, and GOK03) along a continuous 2.3 km long road section south of Esence village exposing sheeted dykes (Table 1 and Figure 2b). Dykes, along the entire outcrop are steeply dipping to the northwest, are ~100 cm thick on average and show clear chilled margins mainly on one side of each dyke.

3.1.4. Troodos Ophiolite

The Troodos ophiolite of Cyprus is one of the world's best preserved and most complete ophiolites [e.g., *Moores and Vine*, 1971; *Moores et al.*, 1984; *Robertson and Xenophontos*, 1993]. The ophiolitic crust formed in the Late Cretaceous (U-Pb age of 92–90 Ma [*Mukasa and Ludden*, 1987]) at a suprasubduction zone spreading center located in a fore-arc position [*Pearce and Robinson*, 2010]. Troodos is the only ophiolite that has been shown to preserve a complete transform-fault bounded ridge segment formed in a suprasubduction zone environment [*Moores and Vine*, 1971; *Simonian and Gass*, 1978; *Varga and Moores*, 1985; *Morris and Maffione*, 2016]. The Troodos ophiolite is one of the type localities of the Penrose-type ophiolite pseudostratigraphy and is deformed into a gentle domal pericline [*Robertson and Xenophontos*, 1993]. In the southwest of Cyprus, the ophiolite is juxtaposed with a chaotic assemblage of magmatic and sedimentary rocks known as Mamonia Complex [e.g., *Robertson and Xenophontos*, 1993]. Juxtaposition of the Troodos ophiolite and the Mamonia Complex occurred between the latest Campanian and the late Maastrichtian (~73–65 Ma) [*Swarbrick and Naylor*, 1980; *Bailey et al.*, 2000].

The sheeted dyke complex is the most extensively exposed unit of the Troodos ophiolite and contains generally steeply dipping dykes striking around a N-S direction [e.g., *Varga and Moores*, 1985; *Bonhommet et al.*, 1988; *Allerton and Vine*, 1991]. Dyke orientations are more variable at the northern and southern edges of the ophiolite, where they rotate toward an ~E-W direction approaching fossil transform faults in the north and south [*Bonhommet et al.*, 1988; *Morris and Maffione*, 2016]. This change in orientation toward the transform zones is ascribed to local dextral shearing during the magmatic spreading phase [e.g., *MacLeod et al.*, 1990; *Morris et al.*, 1990, 1998; *Morris and Maffione*, 2016]. Paleomagnetic data from the ophiolite and its sedimentary cover have demonstrated ~90° of counterclockwise rotation of the ophiolite since its formation [*Clube and Robertson*, 1986; *Morris et al.*, 1990], with most of this large rotation (~65°) occurring prior to the Maastrichtian [*Morris et al.*, 2006]. We will reevaluate the Troodos data in this paper, but this main conclusion remains standing.

3.1.5. Hatay and Baer-Bassit Ophiolites

The Hatay (or Kızıldağ) and Baer-Bassit ophiolites are part of a larger ophiolitic nappe formed in a suprasubduction zone setting [*Whitechurch et al.*, 1984; *Lytwyn and Casey*, 1993; *Parlak et al.*, 2009] and emplaced south to southeastward onto the Arabian platform in the late Maastrichtian [*Tinkler et al.*, 1981; *Piskin et al.*, 1986; *Yılmaz*, 1993; *Al-Riyami and Robertson*, 2002; *Al-Riyami et al.*, 2002; *Inwood et al.*, 2009b]. The Hatay ophiolite in the north represents an ~7 km thick and relatively undeformed slice of oceanic lithosphere showing all

elements of the Penrose ophiolitic sequence, including harzburgites, gabbros, sheeted dykes, and volcanics [*Delaloye et al.*, 1980; *Al-Riyami and Robertson*, 2002]. The sheeted dyke complex is particularly well exposed along a 4.5 km long continuous section where dykes are subvertical and ~E-W striking [*Inwood et al.*, 2009a]. The Baer-Bassit ophiolite in the South forms the leading edge of the emplaced oceanic sheet. It is intensely dismembered, yet still contains a fairly complete Penrose pseudostratigraphy. The sheeted dyke complex is well developed, with dykes steeply dipping and trending mainly NW-SE [*Morris et al.*, 2002]. The volcanic sequence of the ophiolite is uncomformably covered by upper Maastrichtian-Paleogene marine sediments [*Dilek and Delaloye*, 1992; *Al-Riyami et al.*, 2002; *Al-Riyami and Robertson*, 2002].

U-Pb ages on zircons of ~92 Ma from plagiogranite and cumulate gabbro, and Sm-Nd ages of ~95 Ma from gabbro have been reported from the Hatay ophiolite [*Karaoğlan et al.*, 2012]. There is no direct age for the crustal section of the Baer-Bassit ophiolite. ^{40}Ar-^{39}Ar ages on hornblende of 88.9 ± 0.8 Ma from the metamorphic sole beneath the Baer-Bassit ophiolite [*Chan et al.*, 2007] are consistent with other metamorphic sole ages from the Hatay and surrounding ophiolites. Based on these similarities, a Late Cretaceous crustal age for the Baer-Bassit ophiolite is generally assumed.

3.2. Paleomagnetic Analyses

Standard paleomagnetic cores were collected in 2013 and 2014 with a water-cooled portable rock drill and oriented in situ with both magnetic and Sun compasses. All field measurements were corrected for the local magnetic declination (~5°E at the sampled localities; www.ngdc.noaa.gov). Remanence components were analyzed by using mainly stepwise alternating field (AF) demagnetization treatments (2 to 100 mT), with ~10% of the samples at each site demagnetized thermally (up to 580°C, or until complete demagnetization). AF demagnetization and simultaneous measurements of remanences were carried out by using a robotized superconducting (SQUID) cryogenic magnetometer installed at the Paleomagnetic laboratory "Fort Hoofddijk" at Utrecht University, Netherlands. Thermal demagnetizations were carried out by using a shielded oven, with the remanence at each step measured with a cryogenic magnetometer. Demagnetization data were plotted on orthogonal diagrams [*Zijderveld*, 1967], and remanence components were isolated via principal component analysis [*Kirschvink*, 1980] using online software for paleomagnetic data analysis [www.paleomagnetism.org [*Koymans et al.*, 2016]. Calculated characteristic remanent magnetization components (ChRMs) with maximum angle of deviation [*Kirschvink*, 1980] larger than 15° were discarded. Site mean directions were computed by using Fisherian statistics [*Fisher*, 1953] on virtual geomagnetic poles (VGPs) correspondent to the isolated ChRMs, and a fixed 45° cutoff to their distribution [*Johnson et al.*, 2008] was applied. Following the approach of *Deenen et al.* [2011], VGP scatters at each site (approximated by the A_{95} parameter; see Table 1) were used to assess whether paleosecular variation (PSV) of the geomagnetic field was represented at each site. Underrepresentation of PSV (i.e., $A_{95} < A_{95\mathrm{min}}$) in magmatic rocks may indicate either rapid cooling or remagnetization; overrepresentation of PSV (i.e., $A_{95} > A_{95\mathrm{max}}$) indicates significant sources of scatter superimposed on PSV, e.g., due to pervasive deformation at the outcrop scale or an inefficient preservation of the remanence.

3.3. Rock Magnetism and Petrology

To study the nature of the carriers of magnetization, we have analyzed the thermal variation of magnetic susceptibility and Curie temperatures in representative samples. Thermal variation of magnetic susceptibility was measured with an AGICO KLY-3 Kappabridge coupled with a CS3 apparatus during heating-cooling cycles from room temperature to 700°C. The Curie temperatures were investigated with a horizontal translation Curie balance [*Mullender et al.*, 1993] during stepwise heating-cooling cycles from room temperature up to 700°C.

Analyses on polished thin sections using an optical microscope were also carried out to identify microstructures and bulk mineralogical assemblages. The nature and distribution of the ferromagnetic minerals was assessed by using backscattered electron images and elemental analyses using a JEOL JCM-6000 scanning electron microscope coupled with an energy-dispersive X-ray (EDX) (Utrecht University).

3.4. Net Tectonic Rotation Analysis

In standard paleomagnetic studies, deformation is decomposed into a tilt and a vertical-axis rotation. To obtain the vertical-axis rotation component, tilt is first removed by restoring paleo-surfaces back to their original horizontal position (or vertical in case of dykes). Our analysis of paleo-ridge orientations and spreading directions, however, is based on data from sheeted dykes that are generally assumed to have been

intruded in a vertical orientation. Simply restoring dykes to a vertical position, however, is insufficient to correct for the effect of postemplacement tilting because components of tilting around dyke-normal axes produce a change in the initial dyke strike that cannot be resolved. Net tectonic rotation analysis [*Allerton and Vine*, 1987] has been demonstrated to be an effective approach to overcome this problem [*Morris et al.*, 1990, 1998, 2002; *Hurst et al.*, 1992; *Inwood et al.*, 2009a; *Maffione et al.*, 2015b; *Morris and Maffione*, 2016; *van Hinsbergen et al.*, 2016].

Net tectonic rotation analysis calculates the net rotation around an inclined axis that simultaneously brings (i) the paleo-surface from its original (vertical or horizontal) position to the postdeformation orientation as measured in the field and (ii) the direction of the geomagnetic field at the time of ophiolite formation (i.e., the "reference direction") to the calculated in situ site mean paleomagnetic direction. This reference direction is directed due north (or south, in a reversed field) and has an inclination that corresponds to the expected latitude from, e.g., plate tectonic reconstructions, or to the inclination of a tilt corrected paleomagnetic direction from the ophiolite's volcano-sedimentary cover. Net tectonic rotation solutions are expressed as the azimuth and plunge of the rotation axis, the magnitude and sense of rotation, and the initial orientation of the paleo-surface. When applied to dykes, up to two sets of net tectonic rotation solutions can be obtained, depending on whether the dykes can be restored to vertical or not (if they cannot, this may indicate that the dykes did not intrude vertically). If two solutions are obtained, additional geological constraints should be considered to choose a preferred solution. Net tectonic rotation parameters from a single solution should be rejected as they are biased by the selected reference direction (e.g., the initial dyke orientation will always strike perpendicular to the chosen reference direction). Uncertainties on the reference direction, site mean direction, and dyke orientation at each site are modeled by using a method devised by *Morris et al.* [1998], implemented on www.paleomagnetism.org, with modifications listed in *Koymans et al.* [2016], who updated the method to impose no error on the declination of the reference direction, and to use the error on remanence declination and inclination ΔD_x and ΔI_x, instead of the α_{95}. This results in three input vectors for the reference direction (mean value plus two at the edge of the error bar) and five for the in situ dyke orientation and the site mean direction (mean value plus four points along the confidence ellipse). The possible combinations of these vectors generate 75 ($5 \times 5 \times 3$) permissible net tectonic rotation solutions at each site. Combining multiple sites within an ophiolite then leads to a range of potential dyke orientations, which is expressed as the average plus standard deviation.

Here we use the net tectonic rotation analysis to determine rotation parameters and initial orientations of sheeted dykes from the Divriği, Göksun, and Alihoca ophiolites based on our new paleomagnetic data, and on published data from the Troodos [*Bonhommet et al.*, 1988; *Morris et al.*, 1990, 1998, 2002; *MacLeod et al.*, 1990; *Morris and Maffione*, 2016], Hatay, and Baer-Bassit [*Morris et al.*, 2002; *Inwood et al.*, 2009a] ophiolites. In particular, new mean directions were calculated for the Baer-Bassit ophiolite (Table 1) by parametric sampling of site means reported by *Morris et al.* [2002] and performing the analysis on the resulting directions.

In our analysis, the reference direction has a declination (D_{ref}) = 000°, assuming a normal magnetic polarity (all ophiolites formed during the Cretaceous Normal Superchron, 126–83 Ma [*Gradstein et al.*, 2012]). This implies that the net rotation calculated at each site arises from a combination of plate motion and deformation. The inclination (I) of the reference direction for the Turkish ophiolites was determined from paleolatitude estimates based on paleogeographic reconstructions [*van Hinsbergen et al.*, 2016] placed in the paleomagnetic reference frame of *Torsvik et al.* [2012]. Uncertainties on the inclination of the reference direction are related to the reconstructed width of the Neo-Tethys Ocean and the A_{95} error of the reference global apparent polar wander path. According to paleogeographic reconstructions, in the Late Cretaceous (100–90 Ma), the northern branch of the Neo-Tethys Ocean was located between ~33 ± 3°N (southern margin of Eurasia) and ~16 ± 3°N (northern margin of Gondwana). We have no independent paleomagnetic control on the paleolatitudes of the Turkish ophiolites we studied, and we made no a priori assumptions for the location of subduction initiation. We therefore used a 24.5 ± 11.5°N paleolatitude as reference, corresponding to a reference inclination I_{ref} = 40.2° ± 15.4°.

As a reference direction for the Troodos ophiolite we used the inclination of the "Troodos Magnetization Vector" (D = 274°, I = 36.0° ± 7.0° [*Clube and Robertson*, 1986]) and a normal polarity, giving a D_{ref} = 000° and I_{ref} = 36.0° ± 7.0°. Similarly, for the Hatay ophiolite we used the mean inclination from tilt corrected lavas and layered gabbros [*Inwood et al.*, 2009a], providing a reference direction of D_{ref} = 000°, I_{ref} = 32.4° ± 4.5°.

This reference direction has also been applied to the adjacent Baer-Bassit ophiolite, whose crustal section also records some negative inclinations [*Morris et al.*, 2002] that are at odds with a primary magnetization acquired during the Cretaceous Normal Superchron).

4. Results

4.1. Optical Microscope Observations

Optical microscope (transmitted light) observations of thin sections from representative samples of the Divriği, Alihoca, and Göksun ophiolites (two thin sections per ophiolite) identified a mineralogical assemblage composed of plagioclase, clinopyroxene, chlorite, and opaque minerals (Figure 3). In samples from the Göksun and Alihoca ophiolites strongly pleochroic amphiboles (likely hornblende) were also commonly observed. Plagioclase is predominant (~70%) in samples from the Göksun and Divriği ophiolites. Texture is ophitic in samples from the Göksun and Alihoca ophiolites, with large (approximately tens of micrometer) pyroxenes within a matrix of plagioclase, while it is relatively equigranular in samples from the Divriği ophiolite (Figure 3). The internal fabric of all samples is isotropic.

Scanning electron microscope (SEM) observations coupled with EDX analyses (Figure 3) show the occurrence of abundant magnetite grains with size ranging between ~10 and 100 μm, homogeneously dispersed within the silicate matrix (at Divriği and Göksun), or forming ~100 μm large aggregates (at Alihoca). Magnetite grains of ~0.5 μm, and even smaller, were identified in samples from the Divriği and Göksun ophiolites. In samples from the Divriği ophiolite, the smaller grains are titanium-rich titanomagnetite (Figure 3).

Based on these analyses, we conclude that the dykes suffered only low-grade metamorphism under greenschist facies conditions, likely due to seafloor hydrothermal alteration during (or soon after) magmatic activity at the spreading axis.

4.2. Rock Magnetism

Curie balance experiments, thermal variation of magnetic susceptibility, and thermal demagnetization experiments (Figure 4) revealed a predominant Curie temperature of ~580°C in all analyzed samples, consistent with the occurrence of stoichiometric magnetite [*Dunlop and Özdemir*, 1997]. Minor unblocking between 350 and 580°C is consistent with the occurrence of a small fraction represented by titanomagnetite [*Dunlop and Özdemir*, 1997]. Effective removal of the remanence via AF demagnetization supports the occurrence of low-coercivity magnetic minerals, like magnetite and titanomagnetite. Incomplete AF demagnetization of a few specimens (sites DIV04 and DIV07) likely reflects partial low-temperature oxidation (i.e., maghemitization [e.g., *Prévot et al.*, 1981; *Özdemir*, 1990]) of original (titano)magnetite. Generally, straight to concave-upward AF demagnetization decay paths indicate low-to-medium coercivity grains, consistent with a mixture of single-domain and multidomain magnetic grains [*Dunlop and Özdemir*, 1997].

4.3. Paleomagnetism and Net Tectonic Rotation Analysis

4.3.1. Divriği Ophiolite

Magnetic remanences of 151 samples from seven sites from the Divriği ophiolite were analyzed by using AF and thermal treatment, and the results are listed in Table 1. Remanence of the analyzed samples is composed of one or two components of magnetization (Figure 5). When present, a low-stability component was removed at 5–10 mT. Components interpreted as the Characteristic Remanent Magnetization (ChRM) were isolated by demagnetization to 70–80 mT or 580°C. Their distribution is consistent with a PSV-induced scatter (in the sense of *Deenen et al.* [2011]) at six out of seven sites (Table 1). Underrepresentation of PSV at site DIV03 is interpreted to reflect fast cooling of dykes after intrusion, rather than remagnetization, and the direction of magnetization at this site was treated as a single spot reading of the geomagnetic field at the time of emplacement.

Site mean directions (in situ coordinates) have a general northwestward declination and variable inclination, which is substantially different from the present-day geocentric axial dipole (GAD) field direction at the sampling locality (D = 000°, I = 59°), excluding recent remagnetization (Figure 6). A mean remanence direction and dyke orientation was calculated for sites by combining similar results from sites DIV01, DIV02, DIV03, and DIV06, which came from a relatively small area with dykes in similar orientations (Figure 6 and Table 1).

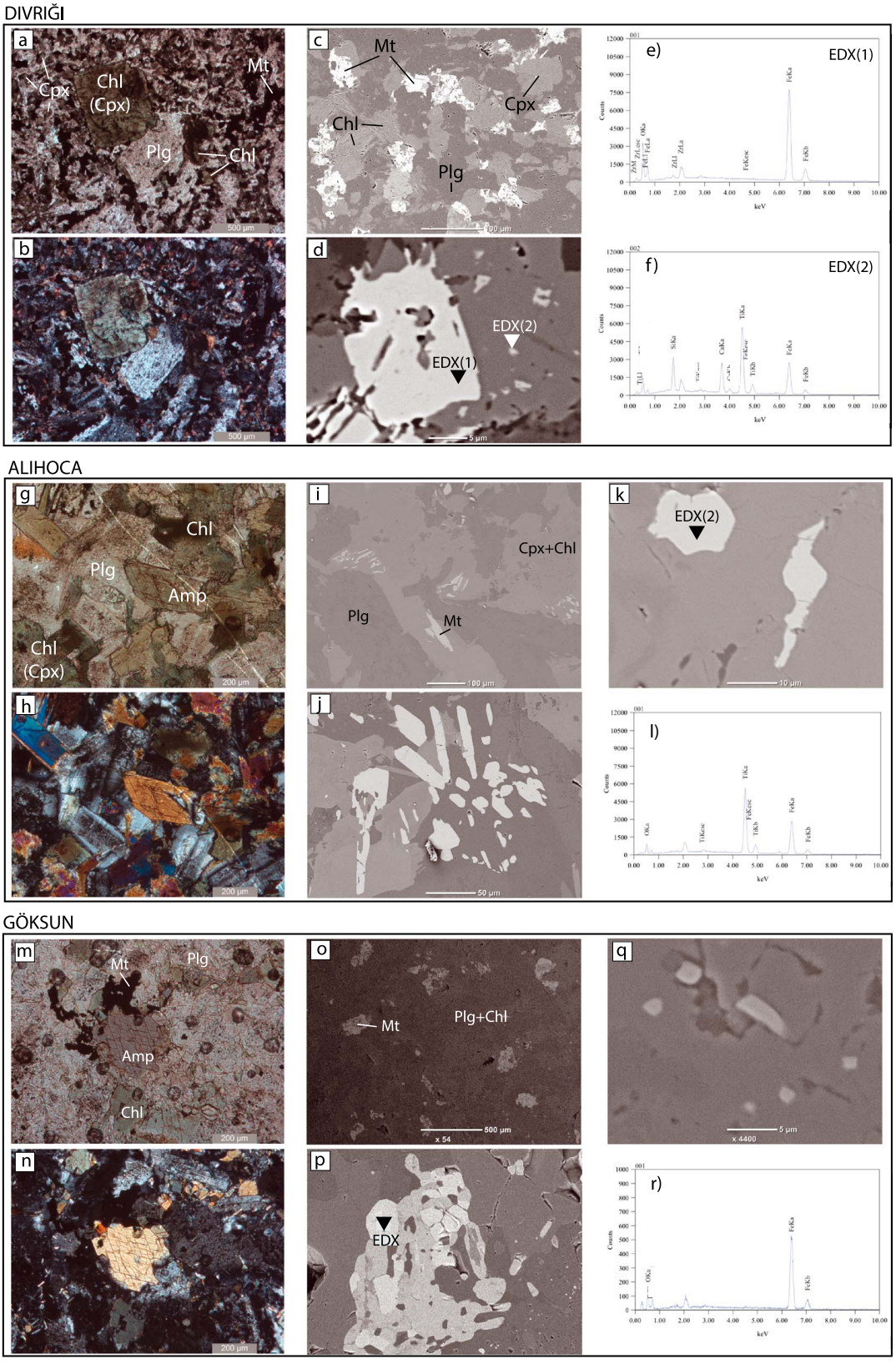

Figure 3. Photomicrographs of three representative thin sections from the Divriği, Alihoca, and Göksun ophiolites analyzed at the optical microscope under (a, g, and m) normal and (b, h, and n) polarized light, and (c, d, i, j, k, o, p, and q) scanning electron microscope (SEM). (e, f, l, and r) EDX elemental analysis graphs of ferromagnetic grains.

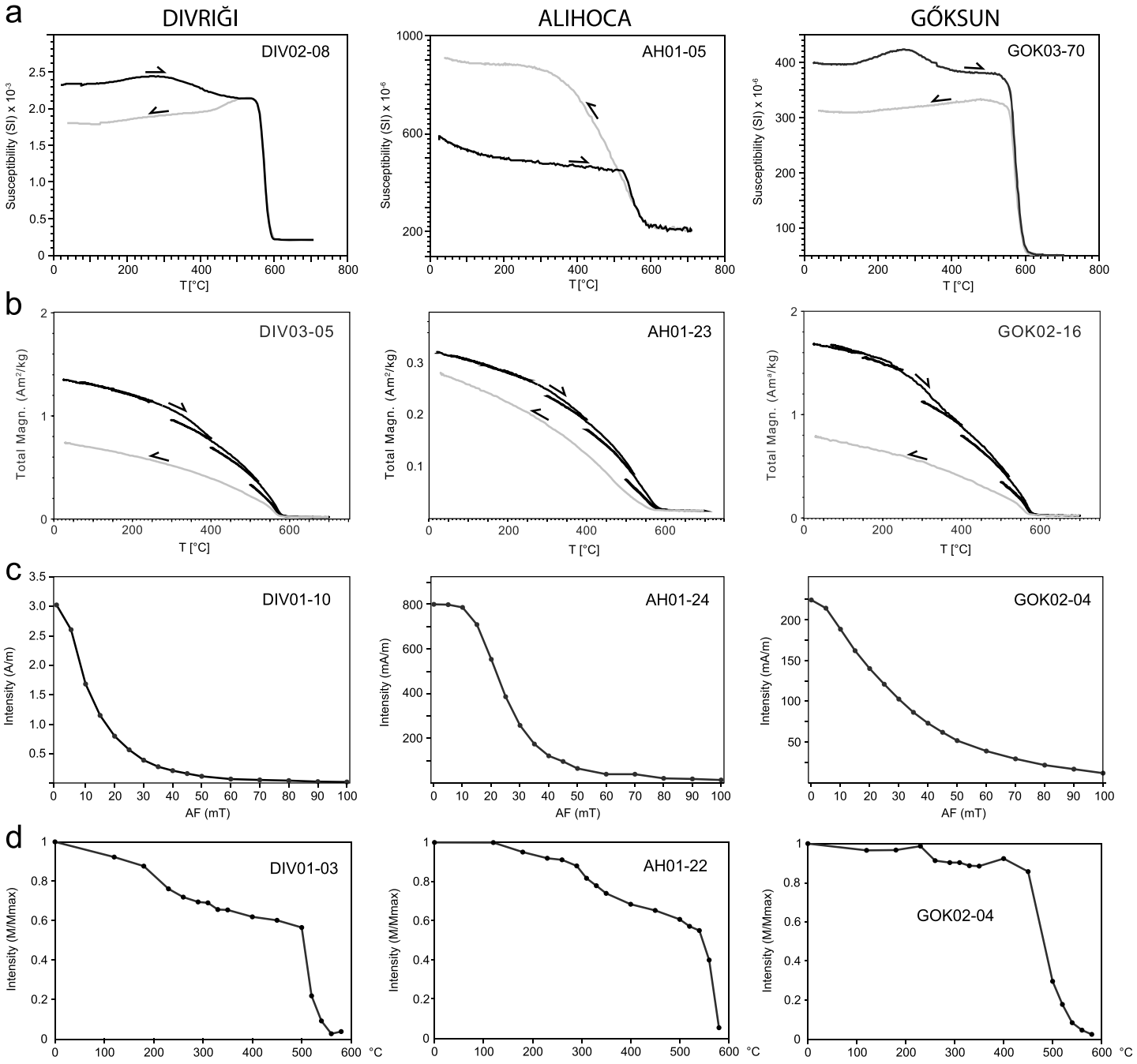

Figure 4. Results from rock magnetic experiments for representative samples from the Divriği, Göksun, and Alihoca ophiolite. (a) Thermal variation of low-field magnetic susceptibility; the black (gray) lines are the heating (cooling) paths. (b) Thermal variation of magnetic remanence during Curie balance experiments; the black (gray) lines are the heating (cooling) paths. (c) Magnetization decay paths during alternating field (AF) demagnetization. (d) Magnetization decay paths (normalized values) during thermal demagnetization.

The net tectonic rotation analysis provided two sets of solutions at all sites (Table 2). The preferred sets of solutions indicate consistent 60–70° rotation around shallowly plunging axes, producing a moderate northeastward tilt consistent with the distribution of the different ophiolitic units in the area, and only minor vertical-axis rotations. Site DIV07 is located several kilometers away form the other sites, and a small variability in the rotation parameters at this site is expected. The combination of permissible solutions (after modeling of uncertainties) obtained at each site or site group provided 300 permissible net tectonic rotation solutions. The initial dyke orientations (preferred solutions) are very consistent and

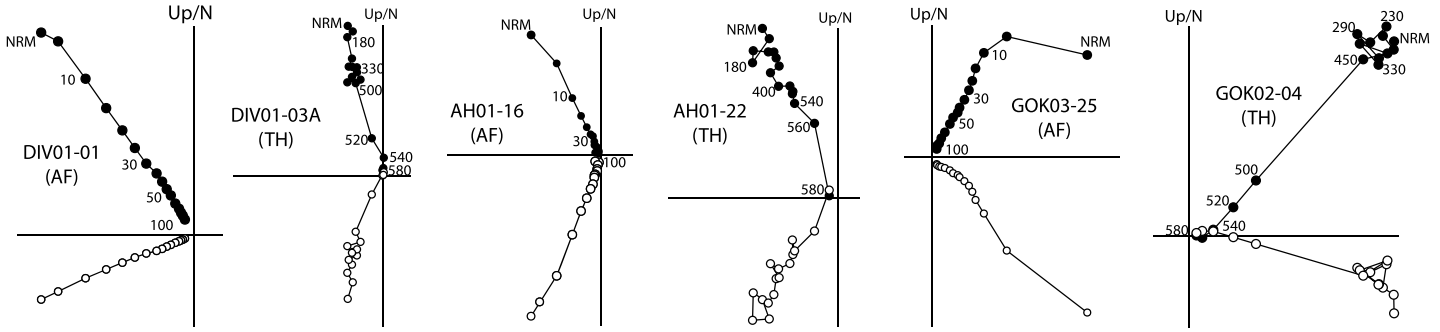

Figure 5. Zijderveld diagrams [*Zijderveld*, 1967] of representative samples demagnetized using thermal (TH) and alternating field (AF) treatment, shown in in situ coordinates. The solid and open dots represent projections on the horizontal and vertical planes, respectively. Demagnetization step values are in °C or in mT.

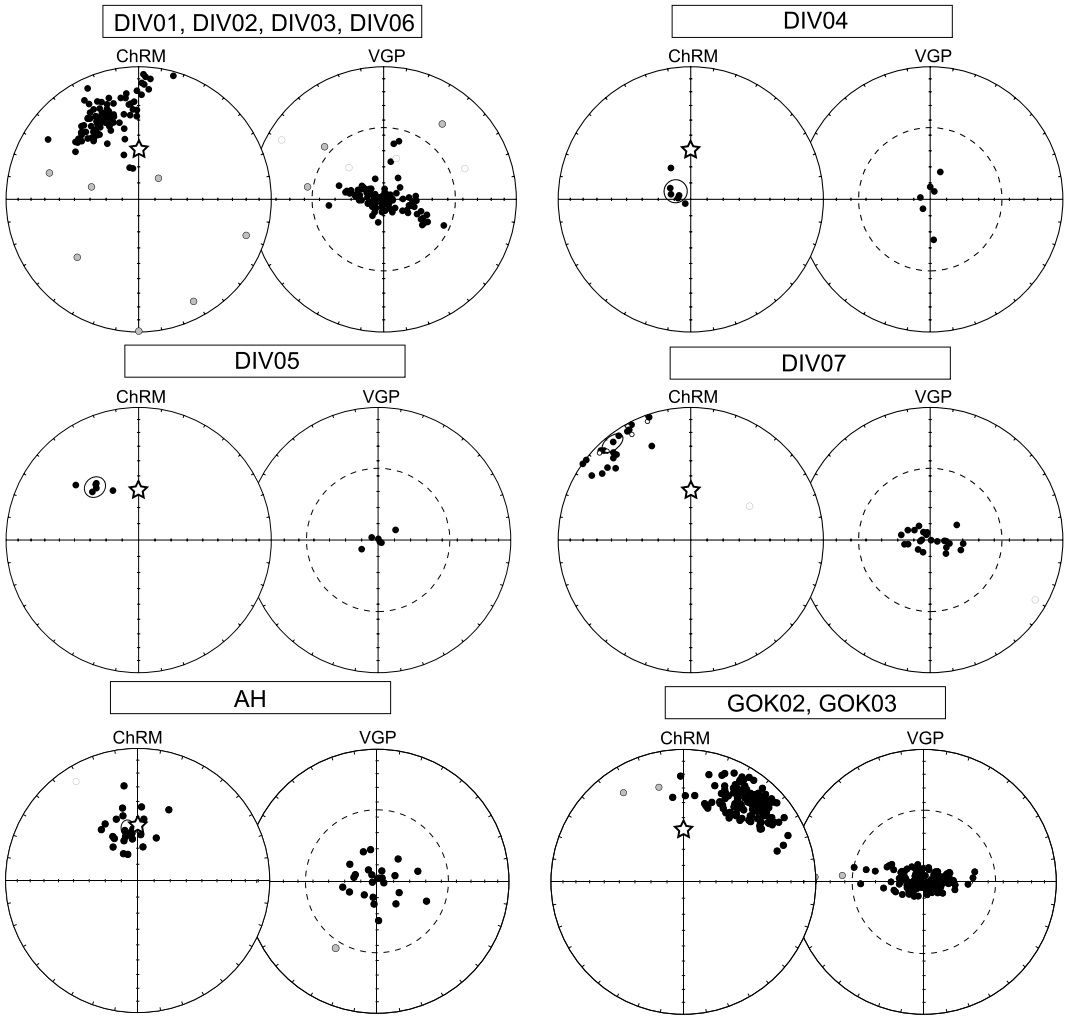

Figure 6. Stereographic projection (lower hemisphere) of the in situ characteristic remanent magnetization (ChRM) directions and corresponding virtual geomagnetic poles (VGPs) for the sampled sites. The grey shaded ellipses are the 95% cones of confidence around the calculated site mean directions. The solid/open dots correspond to normal/reversed magnetic polarity. The grey star indicates the direction of the present-day geocentric axial dipole (GAD) field at the sampling locality (see text). The grey dots are the directions discarded after filtering with a 45° cutoff (represented by the dotted small circles in the VGP plots).

Table 2. Results of the Net Tectonic Rotation Analysis [*Allerton and Vine*, 1987] for the Divriği, Alihoca, and Göksun Ophiolites[a]

	Preferred Solution					Alternate Solution				
	Rotation Axis		Rotation			Rotation Axis		Rotation		
Site	Azimuth	Plunge	Magnitude	Sense	Initial Dyke Strike	Azimuth	Plunge	Magnitude	Sense	Initial Dyke Strike
Divriği										
DIV01/02/03/06	355.7	24.6	67.1	CW	040	335.4	53.0	59.8	CCW	140
DIV04	305.8	38.9	69.9	CW	005	017.6	65.1	122.8	CCW	175
DIV05	337.2	26.8	73.8	CW	026	348.2	63.6	79.0	CCW	154
DIV07	197.9	16.5	57.3	CCW	079	229.3	39.3	49.6	CCW	101
Alihoca										
AH	104.9	12.7	16.9	CCW	017	358.1	50.5	156.8	CCW	163
Göksun										
GOK02/03	113.2	62.9	42.5	CW	020	017.0	27.1	135.5	CCW	160

[a]Both preferred and alternate solutions are shown. Each solution is expressed as azimuth and plunge of the rotation axis, rotation magnitude and sense of rotation, and initial dyke strike.

strike NNE-SSW, indicating an original WNW-ESE spreading direction (Figure 7 and Table 2). The alternate sets of solutions have been discarded due to extreme between-site variability of the rotation magnitude (from ~50° to ~120°).

4.3.2. Alihoca Ophiolite

Well-defined ChRMs were isolated in 26 samples (two samples displayed unstable magnetizations) by demagnetization up to 70–80 mT or 580°C, after removal of low-stability components by treatment at 5–10 mT, or 200°C (Figure 5). Isolated ChRMs are NNW directed and statistically different from the GAD field direction at this locality (D = 000°, I = 56.9°) (Table 1 and Figure 6). VGP scatter is consistent with that induced by PSV [*Deenen et al.*, 2011], consistent with a primary origin of the remanence.

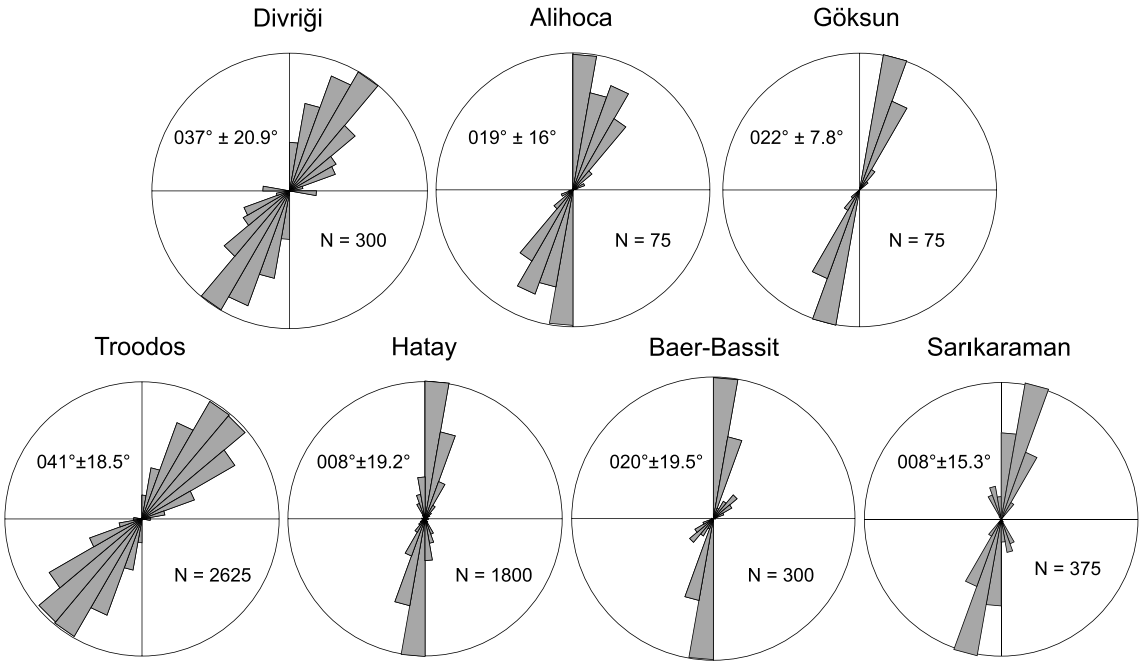

Figure 7. The rose diagram distributions of permissible initial dyke orientations for the studied ophiolites obtained by net tectonic rotation analysis based on the method of *Allerton and Vine* [1987] and modified by *Morris et al.* [1998] and *Koymans et al.* [2016]. Data from the Sarıkaraman ophiolite is reported from *van Hinsbergen et al.* [2016]. The mean dyke strike and relative standard deviation is shown for each ophiolite, together with the number of permissible solutions (n) obtained after modeling of the errors.

Two sets of net tectonic rotation solutions were obtained for the studied section (Table 2). The preferred set of solutions indicates minor counterclockwise rotations around shallowly plunging axes and initial dyke strikes ranging between N-S and NE-SW, consistent with an E-W to NW-SE spreading direction (Figure 7 and Table 2). The alternate set of solutions shows unreasonably large rotations (~160° CCW) around steep axes (Table 2) that are inconsistent with the much smaller counterclockwise rotations documented from this area [*Çinku et al.*, 2016].

4.3.3. Göksun Ophiolite

Paleomagnetic directions were effectively isolated by demagnetization at 80–100 mT or 580°C (Figure 4). Isolated ChRM directions form two clusters: the first one (31 samples) is observed in samples from site GOK01 and is north directed and close to the present-day GAD field direction at the sampling locality (D = 000°, I = 57.5°; Figure 5 and Table 1), indicating probable recent remagnetization. The second cluster (147 samples) is observed in specimens from sites GOK02 and GOK03 and is mainly northeastward directed and with shallow inclinations (Figure 5 and Table 1). Sites GOK02 and GOK03 have been treated as a single site, given their proximity and similar dyke orientations and paleomagnetic directions. These directions are far from the present-day GAD field direction, and recent remagnetization can therefore be excluded. VGP distributions for site GOK02-GOK03 are consistent with a PSV-induced scatter (in the sense of *Deenen et al.* [2011]), and hence compatible with a primary origin of the remanence.

Two sets of net tectonic rotation solutions were obtained by using the mean remanence from site GOK02-GOK03 (Table 2). The preferred set of solutions shows a moderate clockwise rotation around a steep east-plunging axis, indicating the predominance of clockwise vertical-axis rotations over tilt components. The initial dyke strike is N-NNE, compatible with an ~E-W spreading direction (Figure 7 and Table 2). The discarded alternate set of solutions shows a large counterclockwise rotation around a shallowly plunging axis. This would require large tilt of the rock units, approaching overturning, inconsistent with the general structural setting of the ophiolite.

4.3.4. Troodos Ophiolite

Paleospreading directions for the Troodos ophiolite were determined by using a net tectonic rotation analysis based on previously published paleomagnetic data from the sheeted dyke complex [*Bonhommet et al.*, 1988; *Morris et al.*, 1990, 1998; *MacLeod et al.*, 1990; *Morris and Maffione*, 2016]. Single net tectonic rotation solutions were obtained from the nine sites studied by *MacLeod et al.* [1990] and *Morris et al.* [1990] and were therefore discarded. Two sets of solutions were obtained at 35 sites from northwestern Troodos (23 sites from *Morris and Maffione* [2016]), eastern Troodos (9 sites from *Bonhommet et al.* [1988]), and the Akamas peninsula (3 sites exposing "early dykes" from *Morris et al.* [1998]). As preferred solutions we selected those providing large counterclockwise rotations, consistent with the well-constrained paleomagnetic declinations determined from the extrusive sequences and sedimentary cover of the ophiolite [*Clube and Robertson*, 1986]. The 75 permissible preferred solutions (after modeling of uncertainties) from each of the 35 sites were combined providing 2625 permissible solutions for the Troodos sheeted dyke complex. These solutions reveal consistent ~NE-SW initial dyke strikes (Figure 7), from which we infer an ~NW-SE paleospreading direction.

4.3.5. Hatay Ophiolite

Paleospreading directions were calculated for the Hatay ophiolite by using a net tectonic rotation analysis based on published paleomagnetic data from 24 sites within the sheeted dyke complex [*Inwood et al.*, 2009a]. Two sets of solutions were obtained at each site. Modeling of the errors associated with the input vectors of the net tectonic rotation analysis and combining all solutions from the 24 sites produced 1800 permissible net tectonic rotation solutions. The preferred solutions for our analysis were selected in agreement with preferred solutions of *Inwood et al.* [2009a]. These solutions indicate initial ~N-S dyke strikes, corresponding to an approximate E-W paleospreading direction (Figure 7).

4.3.6. Baer-Bassit Ophiolite

Paleospreading directions were calculated for the Baer-Bassit ophiolite by using published paleomagnetic data from the sheeted dyke section (17 sites from *Morris et al.* [2002]), which have been combined into four site groups (Table 1). Two sets of net tectonic rotation solutions have been obtained at each site group, with the preferred solutions chosen following *Morris et al.* [2002]. The combined data set of 300 permissible solutions from the four site groups indicates ~N-S trending initial dyke strikes, consistent with an ~E-W paleospreading direction (Figure 7).

5. Discussion

5.1. Tectonic Meaning of Paleospreading Directions in the Neo-Tethyan Ophiolites

The ophiolites investigated in this study all have a suprasubduction zone geochemical signature [e.g., *Robertson*, 2002, 2004]. Formation of SSZ ophiolites and associated metamorphic soles is widely viewed as intrinsically related to subduction initiation [e.g., *Stern and Bloomer*, 1992; *Dilek and Furnes*, 2011; *Stern et al.*, 2012, *Maffione et al.*, 2015b, *van Hinsbergen et al.*, 2015]. As a consequence, the occurrence of a major Late Cretaceous subduction initiation event within the eastern Mediterranean Neo-Tethys Ocean is now widely accepted [e.g., *Robertson*, 2002, 2004].

The Late Cretaceous Neo-Tethyan ophiolites represent relics of new "fore-arc plates" that grew at new (or reactivated) plate boundaries within the Neo-Tethys above active subduction zones. These fore-arc plates must have been narrow, at least during SSZ spreading, and were bordered by a trench that consumed African plate lithosphere (including the Anatolide-Tauride microcontinental fragment). North of this trench was the other part of the Neo-Tethys Ocean that was already subducting below the Pontides since the Jurassic (the "Anadolu plate" of *Gürer et al.* [2016]). It follows that paleospreading directions from these ophiolites reflect the kinematics of the spreading system of these fore-arc plates located between the new trenches and the Anadolu plate. These kinematics were controlled by the relative motion between the Anadolu plate and the trenches at which African lithosphere subducted, with trench motion driven by motion of the subducted slab relative to the mantle (e.g., roll-back).

Paleospreading direction data obtained from the six ophiolites investigated in this study, plus the Sarıkaraman ophiolite from *van Hinsbergen et al.* [2016], consistently indicate ~N-S to ~NE-SW initial orientations of the ridges from the correspondent SSZ fore-arc plate(s) (Figure 8). Restoring the orientation of the trench adjacent to these spreading centers cannot be constrained directly but requires more circumstantial arguments. Suprasubduction spreading ridges vary between two end-members, i.e., perpendicular to the associated trench and parallel to it [e.g., *Casey and Dewey*, 1984]. Suprasubduction spreading ridges perpendicular to the trench have been proposed for, e.g., the Bela and Muslim Bagh ophiolites of Pakistan [*Gnos et al.*, 1997; *Gaina et al.*, 2015] and the Bay of Island ophiolite [*Dewey and Casey*, 2013]. Suprasubduction spreading ridges parallel to the trench have been proposed for, e.g., the Mirdita ophiolite [*Maffione et al.*, 2015b] and the Izu-Bonin-Mariana fore arc, where basalts and boninites were emplaced at ~50 Ma simultaneously over a $>$500 km long fore arc [*Reagan et al.*, 2010; *Ishizuka et al.*, 2011; *Pearce et al.*, 2015; *Arculus et al.*, 2015].

The regional age distribution of SSZ ophiolites from Turkey, Cyprus, and Syria may provide clues to discriminate between the two end-member scenarios discussed above: SSZ geochemical signatures require that spreading occurred within some 100–150 km from a trench [e.g., *Pearce et al.*, 1984; *Stern et al.*, 2012]. Typical full spreading rates of magmatic spreading centers are of 4–6 cm/yr [e.g., *Müller et al.*, 2008]. At such rates, fore-arc SSZ spreading ridges perpendicular to trenches would produce laterally diachronous ages of SSZ crust in hundreds of kilometers long ophiolite belts like those in the eastern Mediterranean. On the other hand, SSZ spreading ridges parallel to trenches would predict that ophiolites generated at such ridge only during a short period of time (i.e., 1–3 Myr) after the inception of SSZ magmatism. In fact, keeping the trench fixed, any trench-parallel suprasubduction ridge would migrate away from it at half spreading rate, generating back arc rather than SSZ-affinity crust within 4–5 Myr (considering typical full spreading rates of 4–6 cm/yr). The very narrow age range of ~95–90 Ma in which the eastern Mediterranean SSZ ophiolites formed across a geographically wide area thus strongly favors a scenario in which the No-Tethyan trenches were parallel to the suprasubduction spreading centers at which the Upper Cretaceous ophiolites formed.

It follows that the paleospreading directions calculated in this study are consistent with Neo-Tethyan subduction zones striking ~N-S to ~NE-SW. A kinematic restoration of the central Anatolian trench at which the Sarıkaraman ophiolite formed and thrust within ~10 Myr after subduction initiation onto the Kırşehir block further confirms that the intraoceanic trench there was ~N-S striking [*van Hinsbergen et al.*, 2016].

5.2. The Late Cretaceous Geometry of the Subduction System in the Western Neo-Tethys and the Tectonic Evolution of the Eastern Mediterranean Ophiolites

Our new paleospreading direction data from several ophiolites of Turkey, Cyprus, and Syria (Figure 7) indicate that suprasubduction spreading centers formed within the Neo-Tethys above active ~N-S to ~NE-SW oriented subduction segments. This reconstruction, however, is incompatible with current

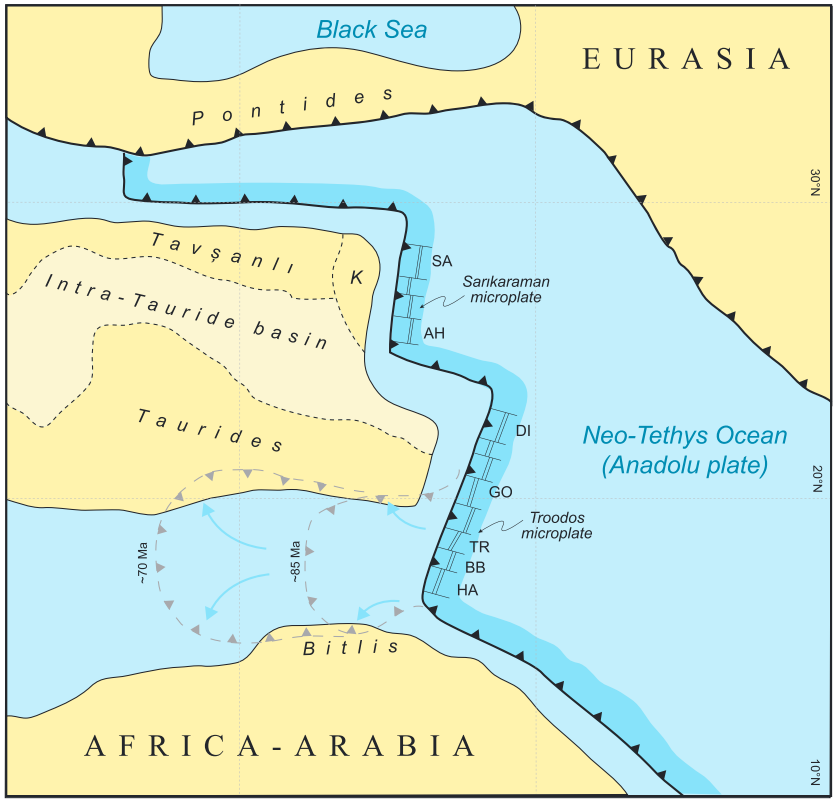

Figure 8. Paleogeographic reconstruction of the eastern Mediterranean Neo-Tethys soon after subduction initiation (~95 Ma) showing the main subduction zones. The dark blue shaded area adjacent to the trench in a fore-arc position indicates the source area of the suprasubduction zone ophiolites. The proposed eastward invasion of the southeastern subduction segment at ~85 and ~70 Ma is shown. The blue arrows indicate the transport directions of ophiolites from the Troodos microplate toward the southern margin of the Tauride (Göksun ophiolite) and the northern margin of Gondwana (Troodos, Baer-Bassit, and Hatay ophiolites). K, Kırşehir block. SA, Sarıkaraman ophiolite. AH, Alihoca ophiolite. DI, Divriği ophiolite. GO, Göksun ophiolite. TR, Troodos ophiolite. BB, Baer-Bassit ophiolite. HA, Hatay ophiolite.

paleogeographic and tectonic models. These used the modern alignment of the Upper Cretaceous ophiolites in the eastern Mediterranean region (forming three E-W trending parallel belts (Figure 1)) to infer that multiple ~E-W trending subduction zones simultaneously formed at preexisting ~E-W trending mid-ocean ridges within the northern and southern Neo-Tethyan strands of the eastern Mediterranean, all accommodating ~N-S convergence between Africa-Arabia and Eurasia during the Late Cretaceous [*Şengör and Yilmaz*, 1981; *Ricou et al.*, 1984; *Whitechurch et al.*, 1984; *Dilek and Delaloye*, 1992; *Lytwyn and Casey*, 1993; *Dilek et al.*, 1999; *Robertson*, 2002; *Moix et al.*, 2008; *Menant et al.*, 2016].

Our new results now require an alternative kinematic model of Late Cretaceous subduction initiation in the Neo-Tethys. Considering the regional distribution of the Neo-Tethyan ophiolites and the documented paleospreading directions, we propose that the Sarıkaraman and Alihoca ophiolites were likely formed above a western ~N-S trending subduction segment, which formed within oceanic lithosphere but close and parallel to the margin of the Kırşehir block (Figure 8). As pointed out by *van Hinsbergen et al.* [2016], subduction must have started within tens of kilometers from the continental margin, since the Central Anatolian ophiolites were thrust southwestward upon the continental margin of the Kırşehir block within ~10 Myr after subduction initiation. Furthermore, considering their present-day location, and their comparable geochemical signature, paleospreading directions, and tectonic rotations, we restore the Divriği, Göksun, Troodos, Hatay, and Baer-Bassit ophiolites altogether along a different, eastern ~N-S to ~NE-SW trending subduction segment, which was likely parallel to the eastern margin of the Tauride block (Figure 8).

The regional ~N-S convergence between Africa-Arabia and Eurasia does not conflict with this configuration; other factors, including buoyancy forces acting on subducting slabs, may in fact control the kinematics of subduction zones and the associated overrriding plate deformation and magmatism. Clear examples of

this can be found in the western Mediterranean where subduction zones formed at low angle to the regional ~N-S Africa-Europe convergence [*Faccenna et al.*, 2001; *Rosenbaum et al.*, 2002]. Further investigations are needed to determine whether the inferred subduction zones of the Neo-Tethys formed spontaneously [*Stern*, 2004] or upon compression [*Gurnis et al.*, 2004] oriented ~E-W.

Based on the major ~90° counterclockwise rotations that were recorded from the Troodos, Hatay, and Baer-Bassit ophiolites [*Morris et al.*, 2002; *Inwood et al.*, 2009a, 2009b], we argue that the southern part of the original N-S trending trench along the eastern Taurides underwent a microplate rotation, consistent with earlier conclusions of, e.g., *Morris et al.* [2002]. We suggest that ophiolites emplaced onto the Bitlis massif, which we associate to the Arabian margin, were also part of this microplate and arrived on the Bitlis margin within ~10 Myr of subduction initiation. This would explain the ~85–80 Ma high-pressure metamorphism in the Bitlis massif [*Oberhänsli et al.*, 2014, 2012]. The Göksun ophiolite also arrived within ~10 Myr after subduction initiation onto continental crust, but in this case of the southeastern Taurides, opposite to the oceanic embayment that separated Arabia and the Taurides. This is consistent with its clockwise rotation documented in this study (Table 1). We thus propose that the original N-S trending subduction zone along the eastern Tauride margin underwent a westward invasion into the eastern Mediterranean embayment involving fast rollback (Figure 8), as previously suggested by *Moix et al.* [2008]. This process would have been similar to that observed, e.g., in the Gibraltar arc [*van Hinsbergen et al.*, 2014] or the Banda arc [*Spakman and Hall*, 2010]. This invasion may also explain the enigmatic tectonic history of the Antalya and Alanya nappes. The Alanya nappes, with their 85–80 Ma HP metamorphism, may have accreted from the easternmost Taurides, at the time the trench hit the SE Tauride margin during Göksun ophiolite emplacement. These Alanya nappes then traveled with the ophiolite far westward and were finally thrust northward over the SW Tauride block, which was experiencing internal thrusting leading to the formation of the Antalya nappes in the latest Cretaceous. The Mersin ophiolite could have also been involved in this invasion process, as suggested by its NW-ward emplacement direction onto the Bolkardag Mesozoic carbonates [*Parlak et al.*, 1996]. The arrest of the invasion is documented by Maastrichtian sediments sealing the frontal thrusts of the Antalya-Alanya nappes and the obduction front of the Baer-Bassit and Hatay ophiolites. The invasion, however, may have endured locally, enabling, e.g., the Troodos ophiolite to continue its intraoceanic rotation until the Eocene [*Morris et al.*, 2006].

Our proposed scenario does not require the simultaneous formation of multiple, in-sequence subduction zones within a relatively small area of the Neo-Tethys as proposed by several models [e.g., *Robertson*, 2002]. Our results are instead consistent with the formation of a single, step-shaped subduction system composed of ~NNE-SSW and ~WNW-ESE segments that may have followed the shape of preexisting continental margins (Figure 8), in agreement with recent studies [*Advokaat et al.*, 2014; *van Hinsbergen et al.*, 2015, 2016]. We propose that the two discrete ~NNE-SSW oriented subduction segments were offset along an ~WNW-ESE oriented fault zone, which initially may have been a transfer fault linking these two trench segments. The ~E-W trending Tauride belt, including HP-LT metamorphic rocks of the Afyon zone [*Pourteau et al.*, 2010], suggests that this fault zone must have developed into a subduction zone itself and likely emplaced ophiolites onto the Taurides (Figure 8). The proposed kinematics represents a snapshot of the initial stage of subduction initiation when ophiolites are formed, and it may have evolved differently after few millions of years when the subduction became self-sustaining. From that time the regional ~N-S convergence between Europe and Africa-Arabia might have played a more central role in the evolution of the subduction zone.

This step-shaped Late Cretaceous subduction zone may have connected to the northwest with the subduction zone below the Pontides through a trench-trench-trench triple junction, as previously suggested by *van Hinsbergen et al.* [2016] (Figure 8). To the east, this subduction zone along the eastern edge of the Tauride platform may eventually have connected further east with the subduction system responsible for the formation of the Oman ophiolite.

5.3. Where did Subduction Start in the Neo-Tethys? A New Kinematic Model of Subduction Initiation in the Neo-Tethys

Previous studies have—logically—argued that intraoceanic subduction zones are likely to initiate at preexisting active intraoceanic plate boundaries: transform faults and (detachment faults along) spreading ridges [e.g., *Gurnis et al.*, 2004; *Maffione et al.*, 2015b; *van Hinsbergen et al.*, 2015]. Our new results, however, seem to point out to a different kinematics incompatible with these widely accepted models. Our new data

rather suggest that the Late Cretaceous subduction system formed parallel to the main continental margins of the Anatolide-Tauride block, which had ~E-W and ~N-S trending segments [*Şengör et al.*, 2008; *van Hinsbergen et al.*, 2016] likely representing a passive margin offset by fracture zones (Figure 8). It is, in fact, unlikely that an active Neo-Tethyan ridge was present so close to these continental margins in the Late Cretaceous, as ophiolite emplacement age constraints would require. Upon northward drift of Sakarya toward Eurasia, the Neo-Tethys Ocean opened in the Early Triassic (~245 Ma) as suggested by the oldest radiolarian cherts found in the mélanges below these ophiolites [*Tekin et al.*, 2016]. According to plate kinematic reconstructions, the Neo-Tethys was ~3000 km wide in the Late Cretaceous [*e.g.*, *Gaina et al.*, 2013; *Torsvik and Cocks*, 2016], and since the middle Jurassic it started to be subducted to the north below the Pontides [*Okay et al.*, 2013; *Dokuz et al.*, 2017]. This implies that the Triassic Neo-Tethyan ridge, initially formed close to the northern margin of Gondwana (i.e., Anatolide-Tauride block), must have been some 1500 km north of it by the Middle Jurassic. Given reconstructed Africa-Europe convergence rates [*Seton et al.*, 2012], even without ongoing spreading, this ridge would have long been subducted below the Pontides by the Early Cretaceous. These considerations imply that no active spreading ridge was present in the Neo-Tethys immediately before the Late Cretaceous subduction initiation event (unless a different spreading center formed close to continental margins at some point before Late Cretaceous subduction initiation, for which there is no geological evidence). We therefore rule out the widely accepted idea that Late Cretaceous subduction initiation in the Neo-Tethys started along active intraoceanic plate boundaries [e.g., *Şengör and Yilmaz*, 1981; *Ricou et al.*, 1984; *Robertson*, 2002; *Moix et al.*, 2008; *Menant et al.*, 2016] and propose that lithospheric weaknesses within old (likely Triassic) oceanic lithosphere were instead used to start the Late Cretaceous subduction system.

Because the Neo-Tethys Ocean opened along an approximate N-S direction due to northward migrations of continental blocks detached from the Gondwana landmass [e.g., *Moix et al.*, 2008], the Neo-Tethyan lithosphere must have been cut by ~N-S striking fracture zones (i.e., the inactive parts of a transform fault) offsetting Triassic ~E-W oriented ridge segments. Interpreting our new results in the context of the above considerations, we propose that Late Cretaceous subduction in the Neo-Tethys initiated along ~NNE-SSW trending old fracture zones and (perhaps hyperextended) orthogonal ~WNW-ESE continental margins.

These somewhat unexpected inferences pose new intriguing questions: What are the causes, mechanisms, and required forces to start a new subduction zone along fracture zones within old and cold lithosphere? How can metamorphic soles below the Neo-Tethyan ophiolites, commonly interpreted as a result of subduction initiation below an active spreading ridge to explain their abnormally hot conditions [*Wakabayashi and Dilek*, 2003; *Dewey and Casey*, 2013; *van Hinsbergen et al.*, 2015], form in the absence of such a preexisting heat source? A multidisciplinary array of future studies is needed to address these fundamental questions. For now, we conclude that current concepts of intraoceanic subduction initiation and formation of ophiolitic metamorphic soles cannot explain the kinematic observations and restorations we presented in this paper.

6. Conclusions

1. Our new paleospreading direction analysis indicate that the Divriği, Alihoca, Göksun, Sarikaraman, Troodos, Hatay, and Baer-Bassit ophiolites of Turkey, Cyprus, and Syria formed at ~N-S to ~NE-SW striking suprasubduction spreading centers. Based on these new data and the published age constraints from the ophiolitic crust and underneath metamorphic soles, we propose that ~NNE-SSW striking intraoceanic subduction zones formed within the Neo-Tethys in the Late Cretaceous, i.e., at low angle to the then pertinent Africa-Europe convergence directions. We suggest that these subduction segments were part of a larger step-shaped subduction system composed of ~NNE-SSW and ~WNW-ESE segments that developed along preexisting lithospheric weakness zones within the Neo-Tethys Ocean.
2. Subduction must have started close (~100 km) to the continental margins of the Anatolide-Tauride block, as indicated by the known short time span (~10 Ma) between ophiolite formation at suprasubduction spreading centers and their emplacement.
3. After subduction initiation, ophiolites that formed above the ~NNE-SSW trending subduction zone east of the Taurides invaded the SE Mediterranean ocean as the slab rolled back westward. This led to major

rotations and radial emplacement/motion of ophiolites in the Maastrichtian, southward towards NW Arabia (Cyprus, Hatay, and Baer-Bassit), and northward onto the SW Tauride block (Göksun).

4. At the time of subduction initiation (~95 Ma), the Triassic Neo-Tethyan spreading ridge that formed during fragmentation of Gondwana and subsequently migrated to the north following the drifting of continental blocks would have already been subducted to the north below the Pontides. This implies that the Late Cretaceous Neo-Tethyan subduction system started at lithospheric weakness zones within ancient (Triassic?) lithosphere. Based on our new results, we propose an alternative model where an intra-Neo-Tethyan subduction zone formed along preexisting ~NNE-SSW fracture zone segments (i.e., inactive parts of a transform fault) that were laterally connected along faults parallel to the passive (hyperextended?) margins of the Anatolide-Tauride block. Our alternative scenario calls for further investigations on the mechanisms of subduction initiation along inactive plate boundaries (rather than active, as typically assumed) and the formation of metamorphic soles below ophiolites in the absence of a heat source (i.e., an active spreading ridge).

Acknowledgments

M.M. and D.J.J.vH. acknowledge funding through an ERC Starting grant (to D.J.J. vH., project 306810–SINK) and an NWO VIDI grant (to D.J.J.vH., project 86411004). We are thankful to Nuretdin Kaymakci and Ercan Aldamaz for discussions on Turkish geology and logistical support. We are indebt with Kalijn Peters for field support during one of the sampling campaigns and with Derya Gürer for discussion on the geology of central Anatolia. Comments by two anonymous reviewers greatly helped to improve the original version of the paper. All data presented in this paper are available on request and can be provided by M.M.

References

Advokaat, E. L., D. J. J. van Hinsbergen, N. Kaymakci, R. L. M. Vissers, and B. W. H. Hendriks (2014), Late Cretaceous extension and Palaeogene rotation-related contraction in Central Anatolia recorded in the Ayhan-Büyükkışla basin, *Int. Geol. Rev.*, *56*(15), 1813–1836, doi:10.1080/00206814.2014.954279.

Al-Riyami, K., and A. H. F. Robertson (2002), Mesozoic sedimentary and magmatic evolution of the Arabian continental margin, northern Syria: Evidence from the Baer-Bassit Melange, *Geol. Mag.*, *139*(4), doi:10.1017/S0016756802006660.

Al-Riyami, K., A. Robertson, J. Dixon, and C. Xenophontos (2002), Origin and emplacement of the Late Cretaceous Baer-Bassit ophiolite and its metamorphic sole in NW Syria, *Lithos*, *65*(1–2), 225–260, doi:10.1016/S0024-4937(02)00167-6.

Allerton, S., and F. J. Vine (1987), Spreading structure of the Troodos ophiolite, Cyprus: Some paleomagnetic constraints, *Geology*, *15*, 593–597, doi:10.1130/0091-7613(1987)15<593.

Allerton, S., and F. J. Vine (1991), Spreading evolution of the Troodos ophiolite, Cyprus, *Geology*, *19*(6), 637–640, doi:10.1130/0091-7613(1991)019<0637:SEOTTO>2.3.CO;2.

Arculus, R. J., et al. (2015), A record of spontaneous subduction initiation in the Izu-Bonin-Mariana arc, *Nat. Geosci.*, *8*(9), 728–733, doi:10.1038/ngeo2515.

Bailey, W. R., R. E. Holdsworth, and R. E. Swarbrick (2000), Kinematic history of a reactivated oceanic suture: The Mammonia complex suture zone, SW Cyprus, *J. Geol. Soc. London*, *157*, 1107–1126.

Barrier, E., and B. Vrielynck (2008), MEBE atlas of paleotectonic maps of the Middle East: Commission for the geological map of the world, Paris.

Bonhommet, N., P. Roperch, and F. Calza (1988), Paleomagnetic arguments for block rotations along the Arakapas fault (Cyprus), *Geology*, *16*(5), 422–425, doi:10.1130/0091-7613.

Bortolotti, V., M. Chiari, M. Marroni, L. Pandolfi, G. Principi, and E. Saccani (2013), Geodynamic evolution of ophiolites from Albania and Greece (Dinaric-Hellenic belt): One, two, or more oceanic basins?, *Int. J. Earth Sci.*, *102*(3), 783–811, doi:10.1007/s00531-012-0835-7.

Bozkurt, E., and R. Oberhänsli (2001), Menderes massif (western Turkey): Structural, metamorphic and magmatic evolution—A synthesis, *Int. J. Earth Sci.*, *89*(4), 679–708, doi:10.1007/s005310000173.

Casey, J. F., and J. F. F. Dewey (1984), Initiation of subduction zones along transform and accreting plate boundaries, triple-junction evolution, and forearc spreading centres—Implications for ophiolitic geology and obduction, *Geol. Soc. London Spec. Publ.*, *13*(1), 269–290, doi:10.1144/GSL.SP.1984.013.01.22.

Çelik, Ö. F., M. Delaloye, and G. Feraud (2006), Precise ^{40}Ar– ^{39}Ar ages from the metamorphic sole rocks of the Tauride Belt ophiolites, southern Turkey: Implications for the rapid cooling history, *Geol. Mag.*, *143*(2), 213, doi:10.1017/S0016756805001524.

Çelik, Ö. F., A. Marzoli, R. Marschik, M. Chiaradia, F. Neubauer, and İ. Öz (2011), Early–Middle Jurassic intra-oceanic subduction in the İzmir-Ankara-Erzincan Ocean, northern Turkey, *Tectonophysics*, *509*(1–2), 120–134, doi:10.1016/j.tecto.2011.06.007.

Cetinkaplan, M., A. Pourteau, O. Candan, O. E. Koralay, R. Oberhänsli, A. I. Okay, F. Chen, H. Kozlu, and F. Şengün (2016), P–T–t evolution of eclogite/blueschist facies metamorphism in Alanya massif: Time and space relations with HP event in Bitlis massif, Turkey, *Int. J. Earth Sci.*, *105*, 247–281, doi:10.1007/s00531-014-1092-8.

Chan, G. H.-N., J. Malpas, C. Xenophontos, and C.-H. Lo (2007), Timing of subduction zone metamorphism during the formation and emplacement of Troodos and Baer-Bassit ophiolites: Insights from ^{40}Ar-^{39}Ar geochronology, *Geol. Mag.*, *144*(5), doi:10.1017/S0016756807003792.

Çinku, M. C., Z. M. Hisarli, Y. Yilmaz, B. Ülker, N. Kaya, E. Öksüm, N. Orbay, and Z. Ü. Özbey (2016), The tectonic history of the Niğde-Kirşehir massif and the Taurides since the Late Mesozoic: Paleomagnetic evidence for two-phase orogenic curvature in Central Anatolia, *Tectonics*, *35*, 772–811, doi:10.1002/2015TC003956.

Clube, T. M. M., and A. H. F. Robertson (1986), The palaeorotation of the troodos microplate, cyprus, in the late mesozoic-early cenozoic plate tectonic framework of the eastern Mediterranean, *Surv. Geophys.*, *8*(4), 375–437, doi:10.1007/BF01903949.

Coleman, R. G. (1981), Tectonic setting for ophiolite obduction in Oman, *J. Geophys. Res.*, *86*, 2497–2508, doi:10.1029/JB086iB04p02497.

Çörtük, R. M., Ö. F. Çelik, M. Özkan, S. C. Sherlock, A. Marzoli, İ. E. Altıntaş, and G. Topuz (2016), Origin and geodynamic environments of the metamorphic sole rocks from the İzmir-Ankara-Erzincan suture zone (Tokat, northern Turkey), *Int. Geol. Rev.*, *58*(15), 1–17, doi:10.1080/00206814.2016.1181991.

Deenen, M. H. L., C. G. Langereis, D. J. J. van Hinsbergen, and A. J. Biggin (2011), Geomagnetic secular variation and the statistics of palaeomagnetic directions, *Geophys. J. Int.*, *186*(2), 509–520, doi:10.1111/j.1365-246X.2011.05050.x.

Delaloye, M., H. De Souza, J. J. Wagner, and I. Hedley (1980), Isotopic ages on ophiolites from the eastern Mediterranean, in *Ophiolites: Proceedings of the International Ophiolite Conference, Cyprus*, *Cyprus Geol. Surv. Dep.*, pp. 292–295.

Dewey, J. F. F. (1976), Ophiolite obduction, *Tectonophysics*, *31*(1–2), 93–120, doi:10.1016/0040-1951(76)90169-4.

Dewey, J. F., and J. F. Casey (2013), The sole of an ophiolite: The Ordovician Bay of Islands Complex, Newfoundland, *J, Geol. Soc. London*, *170*(5), 715–722, doi:10.1144/jgs2013-017.

Dilek, Y., and M. Delaloye (1992), Structure of the Kizildag ophiolite, a slow-spread Cretaceous ridge segment north of the Arabian promontory, *Geology*, *20*(1), 19, doi:10.1130/0091-7613(1992)020<0019:SOTKOA>2.3.CO;2.
Dilek, Y., and H. Furnes (2011), Ophiolite genesis and global tectonics: Geochemical and tectonic fingerprinting of ancient oceanic lithosphere, *Geol. Soc. Am. Bull.*, *123*(3–4), 387–411.
Dilek, Y., P. Thy, H. Bradley, and G. Sidsel (1999), Structure and petrolofy of Tauride ophiolites and mafic dike intrusion, *GSA Bull.*, *111*(8), 1192–1216, doi:10.1130/0016-7606(1999)111<1192:SAPOTO>2.3.CO;2.
Dokuz, A., E. Aydınçakır, R. Kandemir, O. Karslı, W. Siebel, A. Sami Derman, and M. Turan (2017), Late Jurassic magmatism and stratigraphy in the eastern Sakarya zone, Turkey: Evidence for the slab breakoff of Paleotethyan oceanic lithosphere, *J. Geol.*, *125*, 1–31.
Dunlop, D. J., and Ö. Özdemir (1997), *Rock Magnetism: Fundamentals and Frontiers*, p. 573, Cambridge Univ. Press, New York.
Faccenna, C., T. W. Becker, F. P. Lucente, L. Jolivet, and F. Rossetti (2001), History of subduction and back-arc extension in the central Mediterranean, *Geophys. J. Int.*, *145*, 809–820.
Fisher, R. A. (1953), Dispersion on a sphere, *Proc. R. Soc. London*, *217*, 295–305.
Gaina, C., T. H. Torsvik, C. Labails, D. van Hinsbergen, S. Werner, and S. Medvedev (2013), The African plate: A history of oceanic crust accretion and subduction since the Jurassic, *Tectonophysics*, *604*, 4–25, doi:10.1016/j.tecto.2013.05.037.
Gaina, C., D. J. J. van Hinsbergen, and W. Spakman (2015), Tectonic interactions between India and Arabia since the Jurassic reconstructed from marine geophysics, ophiolite geology, and seismic tomography, *Tectonics*, *34*, 875–906, doi:10.1002/2014TC003780.
Gautier, P., E. Bozkurt, V. Bosse, E. Hallot, and K. Dirik (2008), Coeval extensional shearing and lateral underflow during Late Cretaceous core complex development in the Niğde massif, Central Anatolia, Turkey, *Tectonics*, *27*, TC1003, doi:10.1029/2006TC002089.
Gnos, E., A. Immenhauser, and T. Peters (1997), Late Cretaceous/early Tertiary convergence between the Indian and Arabian plates recorded in ophiolites and related sediments, *Tectonophysics*, *271*(1), 1–19.
Gradstein, F. M., J. G. Ogg, M. Schmitz, and G. Ogg (Eds.) (2012), *The Geologic Time Scale 2012*, Elsevier.
Gürer, D., D. J. J. van Hinsbergen, L. Matenco, F. Corfu, and A. Cascella (2016), Kinematics of a former oceanic plate of the Neotethys revealed by deformation in the Ulukışla basin (Turkey), *Tectonics*, *35*, 2385–2416, doi:10.1002/2016TC004206.
Gurnis, M., C. Hall, and L. Lavier (2004), Evolving force balance during incipient subduction, *Geochem. Geophys. Geosyst.*, *5*, Q07001, doi:10.1029/2003GC000681.
Hall, C. E., M. Gurnis, M. Sdrolias, L. L. Lavier, and R. D. Müller (2003), Catastrophic initiation of subduction following forced convergence across fracture zones, *Earth Planet. Sci. Lett.*, *212*(1–2), 15–30, doi:10.1016/S0012-821X(03)00242-5.
Hurst, S. D., K. L. Verosub, and E. M. Moores (1992), Paleomagnetic constraints on the formation of the Solea graben, Troodos ophiolite, Cyprus, *Tectonophysics*, *208*(4), 431–445, doi:10.1016/0040-1951(92)90439-D.
Inwood, J., A. Morris, M. W. Anderson, and A. H. F. Robertson (2009a), Neotethyan intraoceanic microplate rotation and variations in spreading axis orientation: Palaeomagnetic evidence from the Hatay ophiolite (southern Turkey), *Earth Planet. Sci. Lett.*, *280*(1–4), 105–117, doi:10.1016/j.epsl.2009.01.021.
Inwood, J., M. W. Anderson, A. Morris, and A. H. F. Robertson (2009b), Successive structural events in the Hatay ophiolite of southeast Turkey: Distinguishing oceanic, emplacement and post-emplacement phases of faulting, *Tectonophysics*, *473*(1–2), 208–222, doi:10.1016/j.tecto.2008.10.037.
Ishizuka, O., K. Tani, M. K. Reagan, K. Kanayama, S. Umino, Y. Harigane, I. Sakamoto, Y. Miyajima, M. Yuasa, and D. J. Dunkley (2011), The timescales of subduction initiation and subsequent evolution of an oceanic island arc, *Earth Planet. Sci. Lett.*, *306*(3–4), 229–240, doi:10.1016/j.epsl.2011.04.006.
Johnson, C. L., et al. (2008), Recent investigations of the 0–5 Ma geomagnetic field recorded by lava flows, *Geochem. Geophys. Geosyst.*, *9*, Q04032, doi:10.1029/2007GC001696.
Kadioglu, Y. K., and Y. Dilek (2010), Structure and geochemistry of the adakitic Horoz granitoid, Bolkar Mountains, south-central Turkey, and its tectonomagmatic evolution, *Int. Geol. Rev.*, *52*(4–6), 505–535.
Karaoğlan, F., O. Parlak, U. Klötzli, M. Thöni, and F. Koller (2012), U-Pb and Sm-Nd geochronology of the Kızıldağ (Hatay, Turkey) ophiolite: Implications for the timing and duration of suprasubduction zone type oceanic crust formation in the southern Neotethys, *Geol. Mag.*, *150*(April), 1–17, doi:10.1017/S0016756812000477.
Karaoğlan, F., O. Parlak, U. Klötzli, M. Thöni, and F. Koller (2013), U-Pb and Sm-Nd geochronology of the ophiolites from the SE Turkey: Implications for the Neotethyan evolution, *Geodin. Acta*, *3111*, 1–16, doi:10.1080/09853111.2013.858948.
Karaoğlan, F., O. Parlak, E. Hejl, F. Neubauer, and U. Klötzli (2016), The temporal evolution of the active margin along the southeast Anatolian orogenic Belt (SE Turkey): Evidence from U-Pb, Ar-Ar and fission track chronology, *Gondwana Res.*, *33*, 190–208, doi:10.1016/j.gr.2015.12.011.
Kaymakcı, N., M. Inceöz, P. Ertepinar, and A. Koç (2010), Late Cretaceous to Recent kinematics of SE Anatolia (Turkey), *Geol. Soc. London Spec. Publ.*, *340*(1), 409–435, doi:10.1144/SP340.18.
Keenan, T. E., J. Encarnación, R. Buchwaldt, D. Fernandez, J. Mattinson, C. Rasoazanamparany, and P. B. Luetkemeyer (2016), Rapid conversion of an oceanic spreading center to a subduction zone inferred from high-precision geochronology, *Proc. Natl. Acad. Sci. U.S.A.*, *113*, 7359–7366.
Kirschvink, J. L. (1980), The least-squares line and plane and the analysis of palaeomagnetic data, *Geophys. J. R. Astron. Soc.*, *62*(3), 699–718.
Koymans, M. R., C. G. Langereis, D. Pastor-Galán, and D. J. J. van Hinsbergen (2016), Paleomagnetism.org: An online multi-platform open source environment for paleomagnetic data analysis, *Comput. Geosci.*, *93*, 127–137.
Lefebvre, C., A. Barnhoorn, D. J. J. van Hinsbergen, N. Kaymakci, and R. L. M. Vissers (2011), Late Cretaceous extensional denudation along a marble detachment fault zone in the Kırşehir massif near Kaman, central Turkey, *J. Struct. Geol.*, *33*(8), 1220–1236, doi:10.1016/j.jsg.2011.06.002.
Lefebvre, C., K. Peters, P. Wehrens, F. M. Brouwer, and H. L. M. Van Roermund (2015), Thermal and extensional exhumation history of a high-temperature crystalline complex (Hırkadağ massif, Central Anatolia), *Lithos*, *238*, 156–173.
Lytwyn, J. N. N., and J. F. F. Casey (1993), The geochemistry and petrogenesis of volcanics and sheeted dikes from the Hatay (Kizildag) ophiolite, southern Turkey: Possible formation with the Troodos ophiolite, Cyprus, along fore-arc spreading centers, *Tectonophysics*, *223*(3–4), 237–272, doi:10.1016/0040-1951(93)90140-F.
MacLeod, C. J., S. Allerton, I. G. Gass, and C. Xenophontos (1990), Structure of a fossil ridgetransform intersection in the Troodos ophiolite, *Nature*, *348*, 717–720, doi:10.1038/348717a0.
Maffione, M., A. Morris, and M. W. Anderson (2013), Recognizing detachment-mode seafloor spreading in the deep geological past, *Sci. Rep.*, *3*, 2336.
Maffione, M., D. J. J. van Hinsbergen, L. M. T. Koornneef, C. Guilmette, K. Hodges, N. Borneman, W. Huang, L. Ding, and P. Kapp (2015a), Forearc hyperextension dismembered the south Tibetan ophiolites, *Geology*, *43*(6), 475–478, doi:10.1130/G36472.1.

Maffione, M., C. Thieulot, D. J. J. van Hinsbergen, A. Morris, O. Plümper, and W. Spakman (2015b), Dynamics of intraoceanic subduction initiation: 1. Oceanic detachment fault inversion and the formation of supra-subduction zone ophiolites, *Geochem. Geophys. Geosyst.*, *16*, 1–18, doi:10.1002/2015GC005745.

Menant, A., L. Jolivet, and B. Vrielynck (2016), Kinematic reconstructions and magmatic evolution illuminating crustal and mantle dynamics of the eastern Mediterranean region since the late Cretaceous, *Tectonophysics*, *675*, 103–140, doi:10.1016/j.tecto.2016.03.007.

Moix, P., L. Beccaletto, H. W. Kozur, C. Hochard, F. Rosselet, and G. M. Stampfli (2008), A new classification of the Turkish terranes and sutures and its implication for the paleotectonic history of the region, *Tectonophysics*, *451*(1–4), 7–39, doi:10.1016/j.tecto.2007.11.044.

Moores, E. F., P. T. Robinson, J. Malpas, and C. Xenophonotos (1984), Model for the origin of the Troodos massif, Cyprus, and other mideast ophiolites, *Geology*, *12*(8), 500–503, doi:10.1130/0091-7613(1984)12<500:MFTOOT>2.0.CO;2.

Moores, E. M., and F. J. Vine (1971), The Troodos massif, Cyprus and other ophiolites as oceanic crust: Evaluation and implications, *Philos. Trans. R. Soc. London A*, *268*(1192), 443–467.

Morris, A., and M. Maffione (2016), Is the Troodos ophiolite (Cyprus) a complete, transform fault-bounded Neotethyan ridge segment?, *Geology*, *44*(3), 199–202, doi:10.1130/G37529.1.

Morris, A., K. M. M. Creer, and A. H. F. Robertson (1990), Palaeomagnetic evidence for clockwise rotations related to dextral shear along the southern Troodos transform fault, Cyprus, *Earth Planet. Sci. Lett.*, *99*(3), 250–262, doi:10.1016/0012-821X(90)90114-D.

Morris, A., M. W. Anderson, and A. H. F. Robertson (1998), Multiple tectonic rotations and transform tectonism in an intraoceanic suture zone, SW Cyprus, *Tectonophysics*, *299*(1–3), 229–253, doi:10.1016/S0040-1951(98)00207-8.

Morris, A., M. W. Anderson, A. H. F. Robertson, and K. Al-Riyami (2002), Extreme tectonic rotations within an eastern Mediterranean ophiolite (Baäer-Bassit, Syria), *Earth Planet. Sci. Lett.*, *202*(2), 247–261, doi:10.1016/S0012-821X(02)00782-3.

Morris, A., M. W. Anderson, J. Inwood, and A. H. F. Robertson (2006), Palaeomagnetic insights into the evolution of Neotethyan oceanic crust in the eastern Mediterranean, *Geol. Soc. London Spec. Publ.*, *260*(1), 351–372, doi:10.1144/gsl.sp.2006.260.01.15.

Mukasa, S. B., and J. N. Ludden (1987), Uranium-lead isotopic ages of plagiogranites from the Troodos ophiolite, Cyprus, and their tectonic significance, *Geology*, *15*(9), 825, doi:10.1130/0091-7613(1987)15<825:UIAOPF>2.0.CO;2.

Mullender, T. A. T., A. J. van Velzen, and M. J. Dekkers (1993), Continuous drift correction and separate identification of ferrimagnetic and paramagnetic contributions in thermomagnetic runs, *Geophys. J. Int.*, *114*, 663–672, doi:10.1111/j.1365-246X.1993.tb06995.x.

Müller, R. D., M. Sdrolias, C. Gaina, and W. R. Roest (2008), Age, spreading rates, and spreading asymmetry of the world's ocean crust, *Geochem. Geophys. Geosyst.*, *9*, Q04006, doi:10.1029/2007GC001743.

Munteanu, I., L. Maţenco, C. Dinu, and S. Cloetingh (2011), Kinematics of back-arc inversion of the western Black Sea basin, *Tectonics*, *30*, TC5004, doi:10.1029/2011TC002865.

Nikishin, A. M., A. I. Okay, O. Tüysüz, A. Demirer, N. Amelin, and E. Petrov (2015), The Black Sea basins structure and history: New model based on new deep penetration regional seismic data. Part 1: Basins structure and fill, *Mar. Pet. Geol.*, *59*, 638–655, doi:10.1016/j.marpetgeo.2014.08.017.

Oberhänsli, R., R. Bousquet, O. Candan, and A. I. Okay (2012), Dating subduction events in east Anatolia, Turkey, *Turk. J. Earth Sci.*, *21*, 1–17, doi:10.3906/yer-1006-26.

Oberhänsli, R., E. Koralay, O. Candan, A. Pourteau, and R. Bousquet (2014), Late Cretaceous eclogitic high-pressure relics in the Bitlis massif, *Geodin. Acta*, *26*(3–4), 175–190, doi:10.1080/09853111.2013.858951.

Okay, A. I. (1986), High-pressure/low-temperature metamorphic rocks of Turkey, *Geol. Soc. Am. Mem.*, *164*, 333–347.

Okay, A. I., and N. Ozgul (1984), HP/LT metamorphism and the structure of the Alanya massif, southern Turkey: An allochthonous composite tectonic sheet, *Geol. Soc. London Spec. Publ.*, *17*(1), 429–439, doi:10.1144/GSL.SP.1984.017.01.30.

Okay, A. I., and D. L. Whitney (2010), Blueschists, eclogites, ophiolites and suture zones in northwest turkey: A review and a field excursion guide, *Ofioliti*, *35*(2), 131–172.

Okay, A. I., D. Altiner, and A. M. Kilic (2014), Triassic limestone, turbidites and serpentinite–the Cimmeride orogeny in the central Pontides, *Geol. Mag.*, *152*(3), 460–479, doi:10.1017/S0016756814000429.

Okay, A. I., A. C. Şengör, and N. Görür (1994), Kinematic history of the opening of the Black Sea and its effect on the surrounding regions, *Geology*, *22*(3), 267–270.

Okay, A. I., G. Sunal, O. Tüysüz, S. Sherlock, M. Keskin, and A. R. C. Kylander-Clark (2013), Low-pressure-high-temperature metamorphism during extension in a Jurassic magmatic arc, central Pontides, Turkey, *J. Metamorph. Geol.*, *32*(1), 49–69, doi:10.1111/jmg.12058.

Özdemir, Ö. (1990), High-temperature hysteresis and thermoremanence of single-domain maghemite, *Phys. Earth Planet. Int.*, *65*(1–2), 125–136.

Parlak, O. (2006), Geodynamic significance of granitoid magmatism in the southeast Anatolian orogen: Geochemical and geochronogical evidence from Göksun–Afşin (Kahramanmaraş, Turkey) region, *Int. J. Earth Sci.*, *95*(4), 609–627, doi:10.1007/s00531-005-0058-2.

Parlak, O., E. Bozkurt, and M. Delaloye (1996), The obduction direction of the Mersin ophiolite: Structural evidence from subophiolitic metamorphics in the central Tauride Belt, southern Turkey, *Int. Geol. Rev.*, *38*(8), 778–786.

Parlak, O., V. Hock, H. Kozlu, and M. Delaloye (2004), Oceanic crust generation in an island arc tectonic setting, SE Anatolian orogenic belt (Turkey), *Geol. Mag.*, *141*(5), 583–603, doi:10.1017/S0016756804009458.

Parlak, O., H. Yilmaz, and D. Boztuğ (2006), Origin and tectonic significance of the metamorphic sole and isolated dykes of the Divriği ophiolite (Sivas, Turkey): Evidence for slab break-off prior to ophiolite emplacement, *Turk. J. Earth Sci.*, *15*(1), 25–45.

Parlak, O., T. Rızaoğlu, U. Bağcı, F. Karaoğlan, and V. Höck (2009), Tectonic significance of the geochemistry and petrology of ophiolites in southeast Anatolia, Turkey, *Tectonophysics*, *473*(1–2), 173–187, doi:10.1016/j.tecto.2008.08.002.

Parlak, O., F. Karaoğlan, T. Rızaoğlu, U. Klötzli, F. Koller, and Z. Billor (2013), U-Pb and ^{40}Ar-^{39}Ar geochronology of the ophiolites and granitoids from the Tauride belt: Implications for the evolution of the inner Tauride suture, *J. Geodyn.*, *65*, 22–37, doi:10.1016/j.jog.2012.06.012.

Pearce, J. A., and P. T. Robinson (2010), The Troodos ophiolitic complex probably formed in a subduction initiation, slab edge setting, *Gondwana Res.*, *18*(1), 60–81, doi:10.1016/j.gr.2009.12.003.

Pearce, J. A., S. J. Lippard, and S. Roberts (1984), Characteristics and tectonic significance of supra-subduction zone ophiolites, *Geol. Soc. London Spec. Publ.*, *16*(1), 77–94, doi:10.1144/GSL.SP.1984.016.01.06.

Pearce, J. A., et al. (2015), Izu-Bonin-Mariana fore arc: Testing subduction initiation and ophiolite models by drilling the outer Izu-Bonin-Mariana fore arc, Integrated Ocean Drilling Program: Preliminary Reports, (352).

Perinçek, D., and H. Kozlu (1984), Stratigraphy and structural relations of the units in the Afsin-Elbistan-Dogansehir region (eastern Taurus), in *Geology of the Taurus Belt*, *Int. Symp.*, pp. 181–198.

Piskin, O., M. Delaloye, H. Selçuk, and J. Wagner (1986), Guide to Hatay geology, SE Turkey, *Ofioliti*, *11*(2), 87–104.

Plunder, A., P. Agard, C. Chopin, and A. I. Okay (2013), Geodynamics of the Tavşanlı zone, western Turkey: Insights into subduction/obduction processes, *Tectonophysics*, *608*, 884–903, doi:10.1016/j.tecto.2013.07.028.

Plunder, A., P. Agard, C. Chopin, M. Soret, A. I. Okay, and H. Whitechurch (2016), Metamorphic sole formation, emplacement and blueschist facies overprint: Early subduction dynamics witnessed by western Turkey ophiolites, *Terra Nova*, *28*(5), 329–339.

Pourteau, A., O. Candan, and R. Oberhänsli (2010), High-pressure metasediments in central Turkey: Constraints on the Neotethyan closure history, *Tectonics*, *29*, TC5004, doi:10.1029/2009TC002650.

Prévot, M., A. Lecaille, and E. A. Mankinen (1981), Magnetic effects of maghemitization of oceanic crust, *J. Geophys. Res.*, *86*, 4009–4020, doi:10.1029/JB086iB05p04009.

Reagan, M. K., et al. (2010), Fore-arc basalts and subduction initiation in the Izu-Bonin-Mariana system, *Geochem. Geophys. Geosyst.*, *11*, Q03X12, doi:10.1029/2009GC002871.

Ricou, L. E., J. Marcoux, and H. Whitechurch (1984), The Mesozoic organizaion of the Taurides: One or several ocean basins?, *Geol. Soc. London Spec. Publ.*, *17*(1), 349–359, doi:10.1144/GSL.SP.1984.017.01.25.

Robertson, A. H. F. (2002), Overview of the genesis and emplacement of Mesozoic ophiolites in the eastern Mediterranean Tethyan region, *Lithos*, *65*(1–2), 1–67, doi:10.1016/S0024-4937(02)00160-3.

Robertson, A. H. F. (2004), Development of concepts concerning the genesis and emplacement of Tethyan ophiolites in the eastern Mediterranean and Oman regions, *Earth Sci. Rev.*, *66*(3–4), 331–387, doi:10.1016/j.earscirev.2004.01.005.

Robertson, A. H. F. (2012), Late Palaeozoic–Cenozoic tectonic development of Greece and Albania in the context of alternative reconstructions of Tethys in the eastern Mediterranean region, *Int. Geol. Rev.*, *54*(4), 373–454, doi:10.1080/00206814.2010.543791.

Robertson, A. H. F., and C. Xenophontos (1993), Development of concepts concerning the Troodos ophiolite and adjacent units in Cyprus, in *Magmatic Processes and Plate Tectonics*, *Geol. Soc. London Spec. Publ., 76*, pp. 85–119, doi:10.1144/GSL.SP.1993.076.01.05.

Robertson, A. H. F., O. Parlak, and T. Ustaömer (2009), Mélange genesis and ophiolite emplacement related to subduction of the northern margin of the Tauride-Anatolide continent, central and western Turkey, *Geol. Soc. London Spec. Publ.*, *311*(1), 9–66, doi:10.1144/SP311.2.

Robertson, A. H. F., K. Tasli, and N. İnan (2012), Evidence from the Kyrenia Range, Cyprus, of the northerly active margin of the southern Neotethys during Late Cretaceous–Early Cenozoic time, *Geol. Mag.*, *149*(2), 264–290, doi:10.1017/S0016756811000677.

Robertson, A. H. F., O. Parlak, Y. Metln, Ö. Vergİlİ, K. Tasli, N. İnan, and H. Soycan (2013), Late Palaeozoic–Cenozoic tectonic development of carbonate platform, margin and oceanic units in the eastern Taurides, Turkey, *Geol. Soc. London Spec. Publ.*, *372*(1), 167–218, doi:10.1144/sp372.16.

Rosenbaum, G., G. S. Lister, and C. Duboz (2002), Reconstruction of the tectonic evolution of the western Mediterranean since the Oligocene, *J. Virtual Explor.*, *8*, doi:10.3809/jvirtex.2002.00053.

Sayıt, K., and M. C. Göncüoglu (2013), Geodynamic evolution of the Karakaya Mélange complex, Turkey: A review of geological and petrological constraints, *J. Geodyn.*, *65*, 56–65, doi:10.1016/j.jog.2012.04.009.

Schmid, S. M., D. Bernoulli, B. Fügenschuh, L. Matenco, S. Schefer, R. Schuster, M. Tischler, and K. Ustaszewski (2008), The Alpine-Carpathian-Dinaridic orogenic system: Correlation and evolution of tectonic units, *Swiss J. Geosci.*, *101*(1), 139–183, doi:10.1007/s00015-008-1247-3.

Searle, M., and J. Cox (1999), Tectonic setting, origin, and obduction of the Oman ophiolite, *Bull. Geol. Soc. Am.*, *111*(1), 104–122, doi:10.1130/0016-7606(1999)111<0104:TSOAOO>2.3.CO;2.

Şengör, A. M. C., and Y. Yilmaz (1981), Tethyan evolution of Turkey: A plate tectonic approach, *Tectonophysics*, *75*, 181–241.

Şengör, A. M. C., M. S. Özeren, M. Keskin, M. Sakınç, A. D. Özbakır, and I. Kayan (2008), Eastern Turkish high plateau as a small Turkic-type orogen: Implications for post-collisional crust-forming processes in Turkic-type orogens, *Earth Sci. Rev.*, *90*, 1–48, doi:10.1016/j.earscirev.2008.05.002.

Simonian, K. T., and I. G. Gass (1978), Arakapas fault belt, Cyprus: A fossil transform fault, *Geol. Soc. Am. Bull.*, *89*(8), 1220–1230.

Sosson, M., et al. (2016), The eastern Black Sea-Caucasus region during the cretaceous: New evidence to constrain its tectonic evolution, *C. R. Geosci.*, *348*(1), 23–32, doi:10.1016/j.crte.2015.11.002.

Spakman, W., and R. Hall (2010), Surface deformation and slab–mantle interaction during Banda arc subduction rollback, *Nat. Geosci.*, *3*(8), 562–566.

Stern, R. J. (2004), Subduction initiation: Spontaneous and induced, *Earth Planet. Sci. Lett.*, *226*, 275–292.

Stern, R. J., and S. H. Bloomer (1992), Subduction zone infancy: Examples from the Eocene Izu-Bonin-Mariana and Jurassic California arcs, *Geol. Soc. Am. Bull.*, *104*(12), 1621–1636, doi:10.1130/0016-7606(1992)104<1621:SZIEFT>2.3.CO;2.

Stern, R. J., M. K. Reagan, O. Ishizuka, Y. Ohara, and S. A. Whattam (2012), To understand subduction initiation, study forearc crust: To understand forearc crust, study ophiolites, *Lithosphere*, 469–483, doi:10.1130/L183.1.

Swarbrick, R. E., and M. A. Naylor (1980), The Kathikas melange, SW Cyprus: Late cretaceous submarine debris flows, *Sedimentology*, *27*(1), 63–78, doi:10.1111/j.1365-3091.1980.tb01158.x.

Tekin, U. K., and M. C. Göncüoğlu (2007), Discovery of the oldest (upper Ladinian to middle Carnian) radiolarian assemblages from the Bornova Flysch zone in western Turkey: Implications for the Neotethyan Izmir-Ankara ocean, *Ofioliti*, *32*, 131–150.

Tekin, U. K., M. C. Göncüoglu, and N. Turhan (2002), First evidence of late Carnian radiolarians from the Izmir–Ankara suture complex, central Sakarya, Turkey: Implications for the opening age of the Izmir–Ankara branch of Neo-Tethys, *Geobios*, *35*, 127–135.

Tekin, U. K., Y. Bedi, C. Okuyucu, M. C. Göncüoglu, and K. Sayit (2016), Radiolarian biochronology of upper Anisian to upper Ladinian (Middle Triassic) blocks and tectonic slices of volcano-sedimentary successions in the Mersin MElange, southern Turkey: New insights for the evolution of Neotethys, *J. Afr. Earth. Sci.*, *124*, 409–426, doi:10.1016/j.jafrearsci.2016.09.039.

Tinkler, C., J. J. Wagner, M. Delaloye, and H. Selçuk (1981), Tectonic history of the Hatay ophiolites (South Turkey) and their relation with the Dead Sea rift, *Tectonophysics*, *72*(1), 23–41.

Topuz, G., G. Göçmengil, Y. Rolland, O. F. Çelik, T. Zack, and A. K. Schmitt (2013), Jurassic accretionary complex and ophiolite from northeast Turkey: No evidence for the Cimmerian continental ribbon, *Geology*, *41*(2), 255–258, doi:10.1130/G33577.1.

Torsvik, T. H., and L. R. M. Cocks (2016) *Earth History and Palaeogeography*, p. 328, Cambridge Univ. Press, Cambridge.

Torsvik, T. H., et al. (2012), Phanerozoic polar wander, palaeogeography and dynamics, *Earth Sci. Rev.*, *114*(3–4), 325–368, doi:10.1016/j.earscirev.2012.06.002.

Toth, J., and M. Gurnis (1998), Dynamics of subduction initiation at preexisting fault zones, *J. Geophys. Res.*, *103*, 18,053–18,067, doi:10.1029/98JB01076.

Uçurum, A. (2000), Geology, geochemistry, and evolution of the Divrigi and Kuluncak Ophiolitic Melanges, with Reference to Serpentinites in East-Central Turkey, *Int. Geol. Rev.*, *42*(2), 172–191, doi:10.1080/00206810009465076.

van Hinsbergen, D. J. J., N. Kaymakci, W. Spakman, and T. H. Torsvik (2010), Reconciling the geological history of western Turkey with plate circuits and mantle tomography, *Earth Planet. Sci. Lett.*, *297*, 674–686, doi:10.1016/j.epsl.2010.07.024.

van Hinsbergen, D. J. J., R. L. M. Vissers, and W. Spakman (2014), Origin and consequences of western Mediterranean subduction, rollback, and slab segmentation, *Tectonics*, *33*, 393–419, doi:10.1002/2013TC003349.

van Hinsbergen, D. J. J., et al. (2015), Dynamics of intraoceanic subduction initiation: 2. Suprasubduction zone ophiolite formation andmetamorphic sole exhumation in context of absolute plate motions, *Geochem. Geophys. Geosyst.*, *16*, 1771–1785, doi:10.1002/2015GC005746.Dynamics.

van Hinsbergen, D. J. J., et al. (2016), Tectonic evolution and paleogeography of the Kırşehir Block and the Central Anatolian ophiolites, Turkey, *Tectonics*, *35*, 983–1014, doi:10.1002/2015TC004018.

Varga, R. J., and E. M. Moores (1985), Spreading structure of the Troodos ophiolite, Cyprus, *Geology*, *13*(12), 846–850, doi:10.1130/0091-7613.

Wakabayashi, J., and Y. Dilek (2003), What constitutes "emplacement" of an ophiolite?: Mechanisms and relationship to subduction initiation and formation of metamorphic soles, *Geol. Soc. London Spec. Publ.*, *218*(1), 427–447, doi:10.1144/GSL.SP.2003.218.01.22.

Whitechurch, H., T. Juteau, and R. Montigny (1984), Role of the eastern Mediterranean ophiolites (Turkey, Syria, Cyprus) in the history of the Neo-Tethys, *Geol. Evol. East. Mediterr.*, *17*, 301–318, doi:10.1144/GSL.SP.1984.017.01.22.

Yilmaz, Y. (1993), New evidence and model on the evolution of the southeast Anatolian orogen, *Geol. Soc. Am. Bull.*, *105*(2), 251–271, doi:10.1130/0016-7606.

Yilmaz, H., and A. Yilmaz (2004), Geology and structural evolution of the Divrigi-Sivas region, *Geol. Bull. Turkey*, *47*, 13–45.

Yilmaz, H., T. Arkal, and A. Yilmaz (2001), Günefl ofiyolitinin jeolojisi [geology of the Günefl ophiolite (Divri.I-Sivas)], *Proceedings of the 54th Geological Congress of Turkey*, pp. 54–65, Ankara, 7–10 May.

Zijderveld, J. D. A. (1967), A. C. Demagnetization of rocks: Analysis of results, in *Methods in Palaeomagnetism*, edited by D. W. Collinson, K. M. Creer, and S. K. Runcorn, pp. 254–286, Elsevier, New York.